JOURNAL OF PETROLOGY | VOLUME 44 | NUMBER 1 | PAGES 113–140 | 2003

Geochemistry of Lavas from the Emperor Seamounts, and the Geochemical Evolution of Hawaiian Magmatism from 85 to 42 Ma

M. REGELOUS*, A. W. HOFMANN, W. ABOUCHAMI AND S. J. G. GALER

MAX-PLANCK INSTITUT FÜR CHEMIE, ABTEILUNG GEOCHEMIE, POSTFACH 3060, 55020 MAINZ, GERMANY

RECEIVED JULY 10, 2001; REVISED TYPESCRIPT ACCEPTED JULY 16, 2002

The Hawaiian–Emperor Seamount Chain (ESC), in the northern Pacific Ocean, was produced during the passage of the Pacific Plate over the Hawaiian hotspot. Major and trace element concentrations and Sr–Nd–Pb isotopic compositions of shield and post-shield lavas from nine of the Emperor Seamounts provide a 43 Myr record of the chemistry of the oldest preserved Hawaiian magmatism during the Late Mesozoic and Early Cenozoic (from 85 to 42 Ma). These data demonstrate that there were large variations in the composition of Hawaiian magmatism over this period. Tholeiitic basalts from Meiji Seamount (85 Ma), at the northernmost end of the ESC, have low concentrations of incompatible trace elements, and unradiogenic Sr isotopic compositions, compared with younger lavas from the volcanoes of the Hawaiian Chain (<43 Ma). Lavas from Detroit Seamount (81 Ma) have highly depleted incompatible trace element and Sr–Nd isotopic compositions, which are similar to those of Pacific mid-ocean ridge basalts. Lavas from the younger Emperor Seamounts (62–42 Ma) have trace element compositions similar to those of lavas from the Hawaiian Islands, but initial $^{87}Sr/^{86}Sr$ ratios extend to lower values. From 81 to 42 Ma there was a systematic increase in $^{87}Sr/^{86}Sr$ of both tholeiitic and alkalic lavas. The age of the oceanic lithosphere at the time of seamount formation decreases northwards along the Emperor Seamount Chain, and the oldest Emperor Seamounts were built upon young, thin lithosphere close to a former spreading centre. However, the inferred distance of the Hawaiian plume from a former spreading centre, and the isotopic compositions of the oldest Emperor lavas appear to rule out plume–ridge interaction as an explanation for their depleted compositions. We suggest that the observed temporal chemical and isotopic variations may instead be due to variations in the degree of melting of a heterogeneous mantle, resulting from differences in the thickness of the oceanic lithosphere upon which the Emperor Seamounts were constructed. During the Cretaceous, when the Hawaiian plume was situated beneath young, thin lithosphere, the degree of melting within the plume was greater, and incompatible trace element depleted, refractory mantle components contributed more to melting.

KEY WORDS: *Emperor Seamounts; Hawaiian plume; lava geochemistry; lithosphere thickness; mantle heterogeneity*

INTRODUCTION

Long-lived, intra-plate oceanic ('hotspot') magmatism is generally thought to be the surface expression of mantle plumes—columns of relatively hot material rising from deeper in the mantle (Morgan, 1971). Geochemical studies of intra-plate magmatism can therefore potentially give insights into the structure and composition of the Earth's deep mantle. Previous studies have shown that the chemical and isotopic compositions of intra-plate oceanic lavas are more diverse than those of lavas from mid-ocean spreading centres, which sample only the uppermost mantle (e.g. Cohen & O'Nions, 1982; White & Hofmann, 1982; Hofmann, 1997). The origin of the chemical and isotopic heterogeneity in intra-plate oceanic lavas is unclear, although subduction of oceanic crust and sediment is probably responsible for generating heterogeneity in the deeper mantle (Hofmann & White, 1982; Hofmann, 1997).

Seamount chains, created when oceanic plates move over mantle plumes, record changes in the composition

*Corresponding author. Present address: Department of Earth Sciences, University of Bristol, Wills Memorial Building, Queens Road, Bristol BS8 1RJ. Tel: + 44 (0)117 954 5235. Fax: +44 (0)117 925 3385. E-mail: m.regelous@bris.ac.uk

of lavas erupted above a single plume over time. The study of temporal changes in the chemistry of intra-plate magmatism can give insights into the thermal and chemical structure of mantle plumes (Class *et al.*, 1993; White *et al.*, 1993; Hauri *et al.*, 1996; Hoernle *et al.*, 2000), the influence of the oceanic lithosphere on the chemistry of intra-plate lavas (Dupuy *et al.*, 1993; Basu & Faggart, 1996; Chauvel *et al.*, 1997), and the dynamics of mantle plume–spreading ridge interaction (Fisk *et al.*, 1989; Gautier *et al.*, 1990; Class *et al.*, 1993; Cheng *et al.*, 1999). In order to use the geochemistry of intra-plate lavas to probe the composition of the deeper mantle, it is important to know the influence of shallow-level processes such as these on the chemistry of oceanic island lavas. In spite of this, there have been few very detailed studies of the temporal geochemical variations among lavas erupted above mantle plumes. The existing data show that along some seamount chains, there are significant, systematic variations in lava chemistry, whereas other hotspots appear to have erupted lavas with very similar composition over long periods of time. For example, the composition of the lavas erupted above the Louisville hotspot in the southern Pacific has changed very little over the past 70 Myr (Cheng *et al.*, 1987). In contrast, lavas from the Kerguelen Plateau, Ninetyeast Ridge and Kerguelen Archipelago in the Indian Ocean, which were erupted above the Kerguelen hotspot between 120 Ma and the present, appear to show temporal changes in trace element and isotope chemistry. The isotopic variations have been attributed both to radioactive decay in the mantle source of the lavas (Class *et al.*, 1993), and to variable proportions of continental lithosphere, depleted upper-mantle and plume source components, perhaps related to variations in the distance of the plume from a former spreading centre (Gautier *et al.*, 1990; Frey & Weis, 1995; Frey *et al.*, 2000). Geochemical variations among lavas from the Reunion hotspot track in the western Indian Ocean (Fisk *et al.*, 1989), and the Easter Seamount Chain in the eastern Pacific (Cheng *et al.*, 1999) have also been explained by variations in the distance from spreading centres. Lavas from several other seamount chains (e.g. the Line Islands and the Society and Austral chains) have variable compositions, but show no systematic chemical change with time (Nakamura & Tatsumoto, 1988; Garcia *et al.*, 1993; Hémond *et al.*, 1994*a*; White & Duncan, 1996).

In this paper, we present the results of a geochemical study of lavas from the Hawaiian–Emperor Seamount Chain (ESC) in the northern Pacific Ocean, which provide a 43 Myr record (from ~85 to 42 Ma) of the geochemistry of the Hawaiian mantle plume. Previous geochemical studies of lavas from the ESC have shown that the trace element and isotopic compositions of the lavas from the oldest, northernmost seamounts differ significantly from those of younger lavas erupted from volcanoes on the Hawaiian Islands (Lanphere *et al.*, 1980; Regelous & Hofmann, 1999; Keller *et al.*, 2000). The existing data also show that the chemical and isotopic variations along the ESC are large compared with most other seamount chains. We therefore carried out a detailed geochemical and isotopic study of lavas from the Emperor Seamounts, to document in detail the temporal variations in Hawaiian magmatism and determine their origin.

GEOCHRONOLOGY AND PETROLOGY OF THE EMPEROR SEAMOUNTS

Active volcanoes on the Hawaiian Islands represent the current site of intra-plate volcanism which, over the past 85 Myr, has built the Hawaiian–Emperor Seamount Chain in the northern Pacific Ocean (Fig. 1). This seamount chain is almost 6000 km long, and is composed of >100 shield volcanoes with a combined volume of over 10^6 km^3 (Bargar & Jackson, 1974).

Although there have been numerous geochemical studies of lavas from the Hawaiian Islands, much less is known about the geochemistry of Hawaiian volcanoes older than 5 Ma, because most are now submerged and are therefore difficult to sample. The Emperor Seamounts are the oldest preserved products of Hawaiian magmatism. Geochronological studies of lavas from these seamounts have shown that the ages of the volcanoes increase progressively northwards, from Daikakuji (42 Ma) to Detroit (81 Ma). Dalrymple *et al.* (1980*b*) reported a minimum K–Ar age of 61·9 ± 5 Ma for Meiji Seamount, although microfossil assemblages in the overlying sediments indicate that the age of Meiji is at least 68–70 Ma (Worsley, 1973). The radiometric age data for Emperor Seamount lavas have been summarized by Clague & Dalrymple (1989).

A wide range of volcanic rock types have been recovered from the ESC. These include tholeiitic and alkalic basalts and their differentiates, and silica-undersaturated lavas such as basanite, nephelinite and nepheline melilitite (Clague & Dalrymple, 1989; Lonsdale *et al.*, 1993). These rock types are similar to those occurring on the Hawaiian Islands. On Suiko and Ojin Seamounts, drilling has recovered alkali basalts overlying tholeiites (Kirkpatrick *et al.*, 1980), and both tholeiitic (shield) and alkalic (post-shield) lavas are present on Detroit, Koko, Yuryaku and Daikakuji Seamounts (Clague & Dalrymple, 1989; Keller *et al.*, 1995). The similarities in volcano morphology, lava petrology, and the stratigraphic distribution of rock types suggest that the volcanoes of the ESC passed through a series of evolutionary stages similar to those of young Hawaiian volcanoes (Clague & Dalrymple, 1989; Lonsdale *et al.*, 1993).

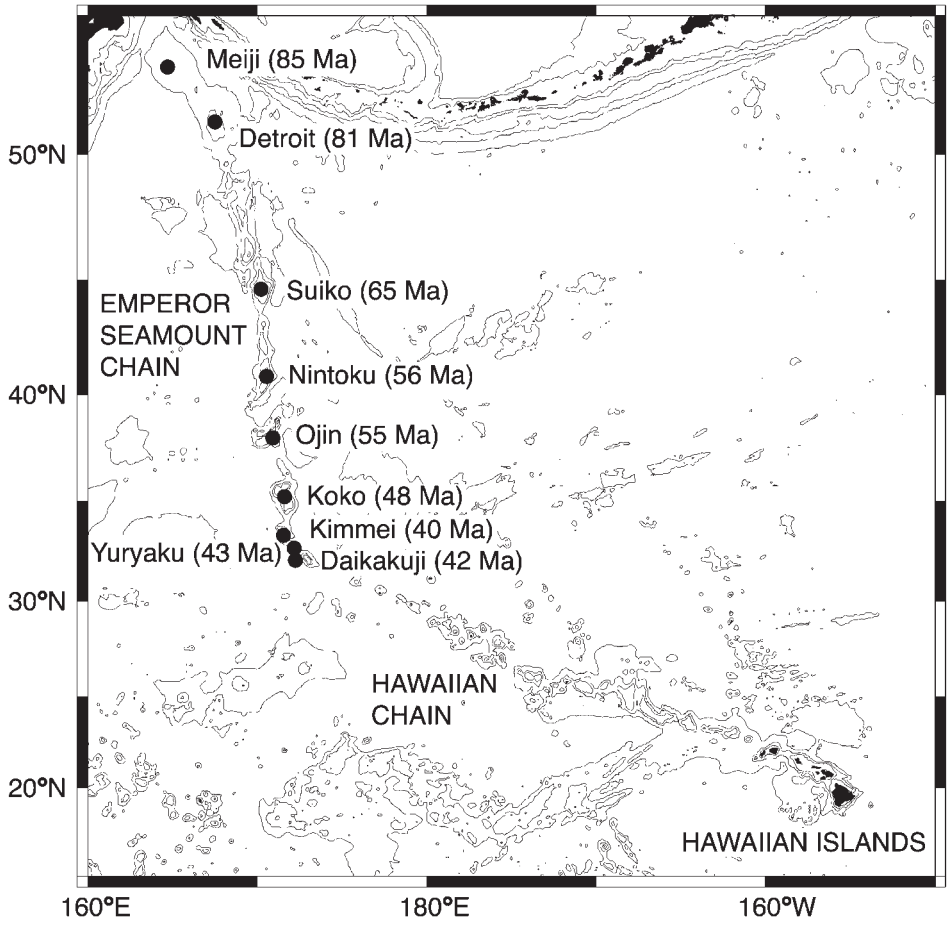

Fig. 1. Bathymetry of the North Pacific (contours at 1500 m intervals), showing the location of the Emperor Seamount Chain and the samples analysed in this study.

Previous studies indicate that lavas from Daikakuji, Yuryaku, Kimmei, Koko, Jingu, Ojin, Nintoku and Suiko Seamounts have major and trace element compositions that are very similar to those of younger lavas from the Hawaiian Islands (Clague & Dalrymple, 1973; Clague *et al.*, 1975; Dalrymple & Clague, 1976; Bence *et al.*, 1980; Clague & Frey, 1980; Dalrymple & Garcia, 1980; Kirkpatrick *et al.*, 1980), and from seamounts along the Hawaiian segment of the Hawaiian–Emperor Chain (Dalrymple *et al.*, 1974, 1981; Garcia *et al.*, 1987). On the other hand, Keller *et al.* (1995) and Regelous & Hofmann (1999) have shown that lavas from Meiji and Detroit Seamounts have lower concentrations of incompatible elements than most lavas from the Hawaiian Islands.

There have been few previous isotopic studies of ESC lavas. Lanphere *et al.* (1980) carried out Sr isotope measurements on lavas from seven of the younger Emperor Seamounts. Those workers showed that tholeiites from the Emperor Seamounts generally have lower age-corrected $^{87}Sr/^{86}Sr$ ratios than tholeiitic lavas from the Hawaiian Islands, and that $^{87}Sr/^{86}Sr$ values decrease northwards along the ESC. Lanphere *et al.* (1980) suggested that this was due to variations in the difference in age between each seamount and the oceanic crust on which it was built. Recent studies of lavas from Meiji and Detroit Seamounts (Keller *et al.*, 2000) have shown that these lavas have more depleted Sr and Nd isotope compositions than all other Hawaiian–Emperor lavas. Keller *et al.* (2000) speculated that this was the result of plume–ridge interaction. Here we present combined major and trace element, and Sr, Nd and Pb isotope data for Emperor Seamount lavas, and show that lavas from the oldest Emperor Seamounts also have depleted incompatible trace element compositions compared with younger Hawaiian–Emperor lavas. We suggest that the chemical and isotopic variations in lavas from the ESC result from differences in the degree of melting of a

heterogeneous mantle, as a result of variations in the thickness of the lithosphere upon which the seamounts were built.

SAMPLE LOCATIONS

We analysed 44 lava samples from nine seamounts along the entire length of the Emperor Seamount Chain (Fig. 1). The samples provide an ~43 Myr record of the geochemistry of Hawaiian magmatism, between ~85 and 42 Ma. Samples from the northern seamounts were collected by drilling, and all dredge samples were collected south of latitude 37°N. None of these samples can therefore represent glacial dropstones, which occur only north of latitude 41°N (Lonsdale *et al.*, 1993). Sample locations are given in Table 1.

Deep Sea Drilling Project (DSDP) Leg 19, Hole 192A, recovered an ~13 m thickness of pillow basalts from near the summit of Meiji Guyot (Stewart *et al.*, 1973). The lavas were initially classified as alkali basalts on the basis of their mineralogy, but subsequent microprobe analyses of glass and pyroxene suggested that they are tholeiitic (Dalrymple *et al.*, 1980*a*). At least five flow units were represented (Stewart *et al.*, 1973). Samples from four flows were selected for analysis in this study.

Drilling at Site 883, Ocean Drilling Program (ODP) Leg 145, on Detroit Seamount penetrated basement and recovered 24 m and 38 m of plagioclase-phyric basalt in two holes located 20 m apart. The lavas were described as transitional in composition (Keller *et al.*, 1995). Six samples from these two holes were analysed in this study. Hole 884E penetrated 87 m into basement, and recovered basaltic pillows and massive flows, which were divided into 13 lithological units. Major and trace element analyses (Keller *et al.*, 1995) showed these to be of tholeiitic composition. Samples from five units were analysed in this study.

During DSDP Leg 55, three holes were drilled into the volcanic basement of Suiko Seamount. A thickness of 11 m of alkali basalt was recovered from Hole 433A, and 19 m (two flow units) of alkali basalt from Hole 433B. Hole 433C penetrated almost 400 m into at least 114 subaerially erupted lava flows consisting of tholeiitic basalt, picrite and overlying alkali basalt (Kirkpatrick *et al.*, 1980). We analysed eight samples from these three holes; an alkali basalt from each of Holes 433A and 433B, and five tholeiitic basalts and an alkali basalt from Hole 433C.

Ojin and Nintoku Seamounts were drilled on DSDP Leg 55. Hole 430A (Ojin Seamount) penetrated 28 m (five flow units) of basalt. Subsequent major element analyses of these rocks showed the lowermost unit to be tholeiitic in composition, whereas the overlying units are hawaiites (Kirkpatrick *et al.*, 1980). Four samples, including the tholeiite, were analysed in this study. Hole 432A (Nintoku Seamount) penetrated 32 m of basement, comprising three flow units of alkali basalt, and an overlying conglomerate containing volcanic cobbles. We analysed samples from each of the three flows, and a hawaiite cobble from the conglomerate previously analysed by Kirkpatrick *et al.* (1980).

We also studied samples that were collected from the southern Emperor Seamounts by dredging during the Scripps Institution of Oceanography cruise AIRES VII, in 1971. This cruise recovered volcanic rocks from Koko, Kimmei, Yuryaku and Daikakuji Seamounts. Major element and some trace element analyses, as well as K–Ar and/or Ar–Ar data for samples from these dredge hauls have been previously reported by Clague and co-workers (Clague & Dalrymple, 1973, 1987; Clague *et al.*, 1975; Dalrymple &d Clague, 1976). Two dredges on Koko Seamount recovered a range of rock types, including tholeiitic and alkalic basalt, hawaiite, mugearite, trachyte and phonolite. Both tholeiitic and alkalic basalts were recovered from Yuryaku, whereas only alkali basalts were dredged from Kimmei and Daikakuji Seamounts. Thirteen of the least altered samples from five dredges from these four seamounts were analysed in this study. The dredge samples are in the form of pebbles and blocks, varying from 5 to 40 cm in diameter, many of which had Fe–Mn coatings. The dredged samples are generally more altered than the drilled samples (Table 1).

ANALYTICAL TECHNIQUES

Dredge samples were crushed to 0·5–2 cm fragments, and material was hand-picked from the interior of the pebbles, to avoid the Fe–Mn coatings on some of these samples. Drill core material was crushed to chips of 2–3 mm size, and the freshest material was hand-picked. The chips were washed twice in distilled water in an ultrasonic bath, dried, and crushed in an agate swing mill. Rock chips for trace element analyses were handpicked to avoid phenocrysts, but several of the samples analysed (e.g. 55-13, 145-10) included olivine or plagioclase phenocryst fragments.

Major element analyses (Table 2) were carried out by X-ray fluorescence (XRF) at the Universität Mainz, Germany. Trace element concentrations (Table 2) were determined by inductively coupled plasma mass spectrometry (ICP-MS) using a Fisons Plasmaquad II instrument at the University of Queensland, Australia. Full details of the procedure have been given by Niu & Batiza (1997). External precision on the concentrations of most of the trace elements measured is between 1 and 3% (Table 2).

Table 1: Age, location and petrography of samples analysed in this study

Sample	Seamount	Age (Ma)	Distance from Kilauea (km)	Latitude	Longitude	Leg-Hole	Core-Section	Interval	Depth (mbsf)	Alteration	Phenocrysts
Drilled samples											
19-1	Meiji	~85	5800	53°00·57′N	164°42·82′E	19-192A	5-3	10–13	1046·10	3	p6, c2
19-2	Meiji	~85	5800	53°00·57′N	164°42·82′E	19-192A	5-3	100–104	1047·00	5	p4, c1
19-3	Meiji	~85	5800	53°00·57′N	164°42·82′E	19-192A	5-4	108–113	1048·58	4	p5, c2
19-4	Meiji	~85	5800	53°00·57′N	164°42·82′E	19-192A	5-6	58–63	1051·08	5	p4
145-1	Detroit	81·0	5580	51°11·92′N	167°46·10′E	145-883E	21R-5	104–108	833·42	5	p3
145-2	Detroit	81·0	5580	51°11·92′N	167°46·10′E	145-883E	21R-6	25–30	834·07	4	p3
145-3	Detroit	81·0	5580	51°11·92′N	167°46·10′E	145-883E	22R-2	47–52	838·43	3	p2
145-4	Detroit	81·0	5580	51°11·90′N	167°46·08′E	145-883F	1R-3	37–41	823·37	5	aphyric
145-5	Detroit	81·0	5580	51°11·90′N	167°46·08′E	145-883F	2R-3	118–122	833·68	5	aphyric
145-6	Detroit	81·0	5580	51°11·90′N	167°46·08′E	145-883F	3R-4	29–33	844·22	3	aphyric
145-7	Detroit	81·0	5580	51°27·03′N	168°20·22′E	145-884E	2R-2	32-–36	854·28	1	aphyric
145-8	Detroit	81·0	5580	51°27·03′N	168°20·22′E	145-884E	6R-3	36–40	894·65	2	aphyric
145-9	Detroit	81·0	5580	51°27·03′N	168°20·22′E	145-884E	9R-1	110–115	911·80	2	p15
145-10	Detroit	81·0	5580	51°27·03′N	168°20·22′E	145-884E	9R-2	70–75	912·78	2	p20, o5
145-11	Detroit	81·0	5580	51°27·03′N	168°20·22′E	145-884E	10R-4	6–10	924·58	2	p30, o7
55-9	Suiko	64·7	4827	44°46·60′N	170°01·26′E	55-433A	20-1	38–43	163·88	2	p12, c8
55-10	Suiko	64·7	4827	44°46·60′N	170°01·23′E	55-433B	5-2	83–88	168·83	2	p10, c5
55-11	Suiko	64·7	4827	44°46·63′N	170°01·23′E	55-433C	4-1	39–44	181·89	2	p8, c4, o3
55-12	Suiko	64·7	4827	44°46·63′N	170°01·23′E	55-433C	15-6	36–40	250·36	3	p3, c2
55-13	Suiko	64·7	4827	44°46·63′N	170°01·23′E	55-433C	24-7	139–144	317·89	2	o30
55-14	Suiko	64·7	4827	44°46·63′N	170°01·23′E	55-433C	28-2	18–24	347·18	4	p6, c2
55-15	Suiko	64·7	4827	44°46·63′N	170°01·23′E	55-433C	28-5	97–102	352·47	3	p6, c3, o2
55-16	Suiko	64·7	4827	44°46·63′N	170°01·23′E	55-433C	31-1	8–14	374·08	3	p3, o8
55-5	Nintoku	56·2	4452	41°20·03′N	170°22·74′E	55-432A	1-1	34–39	36·34	5	p4
55-6	Nintoku	56·2	4452	41°20·03′N	170°22·74′E	55-432A	2-1	80–86	42·3	4	p7, o2
55-7	Nintoku	56·2	4452	41°20·03′N	170°22·74′E	55-432A	2-2	107–112	44·07	3	p6
55-8	Nintoku	56·2	4452	41°20·03′N	170°22·74′E	55-432A	3-2	102–106	57·52	2	p5, o3, c1
55-1	Ojin	55·2	4102	37°59·29′N	170°35·86′E	55·430A	5-2	121–127	69·21	2	aphyric
55-2	Ojin	55·2	4102	37°59·29′N	170°35·86′E	55-430A	6-2	105–111	78·55	1	aphyric
55-3	Ojin	55·2	4102	37°59·29′N	170°35·86′E	55-430A	6-2	131–135	78·81	3	p3
55-4	Ojin	55·2	4102	37°59·29′N	170°35·86′E	55-430A	6-4	142–146	81·92	2	p10, c3

Table 1: continued

Sample	Seamount	Age (Ma)	Distance from Kilauea (km)	Latitude	Longitude	Leg-Hole	Core-Section	Interval	Depth (mbsf)	Alteration	Phenocrysts
	Dredged samples								Depth (mbsl)		
A43D-a	Koko	48·1	3758	34°48·5′N	171°55·5′E				823–624	2	o2
A43D-c	Koko	48·1	3758	34°48·5′N	171°55·5′E				823–624	3	aphyric
A43D-d	Koko	48·1	3758	34°48·5′N	171°55·5′E				823–624	5	p1
A43D-g	Koko	48·1	3758	34°48·5′N	171°55·5′E				823–624	5	p8
A44D-a	Koko	48·1	3758	36°34·6′N	170°57·0′E				1896–1317	5	p2
A44D-b	Koko	48·1	3758	36°34·6′N	170°57·0′E				1896–1317	5	aphyric
A44D-c	Koko	48·1	3758	36°34·6′N	170°57·0′E				1896–1317	5	p2, c2
A51D-a	Kimmei	39·9	3668	33°41·6′N	171°33·1′E				1558–1298	4	p3
A53D-b	Yuryaku	43·4	3520	32°43·2′N	172°12·1′E				947–645	5	o2
A53D-c	Yuryaku	43·4	3520	32°43·2′N	172°12·1′E				947–645	4	aphyric
A55D-b	Daikakuji	42·4	3493	32°08·2′N	172°15·7′E				1360–1259	3	p3, c5
A55D-d	Daikakuji	42·4	3493	32°08·2′N	172°15·7′E				1360–1259	4	p2, c5
A55D-e	Daikakuji	42·4	3493	32°08·2′N	172°15·7′E				1360–1259	4	p5, c1

Phenocryst content (o, olivine; p, plagioclase; c, clinopyroxene) is given in vol. %. Approximate degree of alteration is expressed on a scale of 1–5, where 1 is least altered (unaltered olivine, fresh glass, no secondary minerals), and 5 is most altered (olivine and glass completely replaced, plagioclase partially altered, abundant secondary minerals in vesicles and groundmass). Seamount ages: Detroit from Keller *et al.* (1995); Suiko, Nintoku and Ojin from Dalrymple *et al.* (1980*a*); Koko, Kimmei, Yuryaku and Daikakuji from Clague & Dalrymple (1973), Clague *et al.* (1975) and Dalrymple & Clague (1976).

Table 2: Major and trace element compositions of Emperor–Hawaiian Seamount lavas

Sample:	19-1	19-2	19-3	19-4	145-1	145-2	145-3	145-4	145-5	145-6	145-7	145-8	145-9	145-10	145-11
Seamount:	Meiji	Meiji	Meiji	Meiji	Detroit	Detroit	Detroit	Detroit	Detroit	Detroit	Detroit	Detroit	Detroit	Detroit	Detroit
Rock type:	T	T	T	T	TB	TB	TB	TB	TB	TB	T	T	T	T	T
Stage:	S	S	S	S	PS?	PS?	PS?	PS?	PS?	PS?	S	S	S	S	S
SiO_2	49·47	50·28	50·01	48·18	47·13	47·17	46·65	45·63	45·90	44·64	48·19	48·58	48·63	48·22	48·09
TiO_2	2·11	2·26	2·07	2·11	2·21	2·28	2·15	2·47	2·23	2·53	1·38	1·51	1·24	0·96	1·03
Al_2O_3	15·02	16·05	15·74	14·22	14·94	15·89	15·07	17·69	14·27	17·63	15·24	14·94	16·03	19·94	18·85
Fe_2O_3	11·05	9·23	10·50	14·84	12·60	12·09	12·75	13·61	12·47	13·86	11·65	12·15	10·84	8·52	8·79
MnO	0·15	0·15	0·14	0·17	0·18	0·19	0·16	0·20	0·13	0·21	0·18	0·16	0·15	0·12	0·12
MgO	6·68	6·89	6·83	5·80	7·12	7·16	6·20	1·82	5·65	2·08	8·51	7·51	7·47	6·18	7·18
CaO	11·11	10·06	9·71	9·24	11·62	11·10	13·07	13·41	15·37	13·71	11·95	11·84	12·75	13·69	13·45
Na_2O	3·03	3·14	2·88	2·75	3·01	3·11	3·01	3·48	2·96	3·49	2·63	2·83	2·76	2·56	2·45
K_2O	1·14	1·98	2·04	2·57	0·70	0·54	0·95	1·41	1·18	1·14	0·10	0·13	0·12	0·09	0·12
P_2O_5	0·23	0·23	0·22	0·23	0·25	0·25	0·23	0·45	0·24	0·69	0·10	0·11	0·09	0·06	0·08
LOI	2·45	3·07	2·72	3·62	2·86	2·90	3·98	5·05	5·72	4·39	1·52	0·98	0·43	0·72	0·58
Total	100·00	100·27	100·13	100·12	99·78	99·78	100·23	100·18	100·42	100·00	99·95	99·82	100·09	100·35	100·17
Sc	42·5	41·4	40·9	39·8	38·7	38·4	38·4	41·9	38·4	43·9	48·4	48·76	46·2	35·4	36·6
Ti	12041	13270	11877	12167	12786	13135	12592	14347	12955	14717	8282	9331	7681	6018	6477
V	298	292	303	337	286	292	291	301	292	362	270	303	254	198	206
Cr	84·0	60·4	79·7	61·0	160	165	171	158	160	161	315	293	267	226	270
Co	66·5	53·1	52·7	36·5	45·8	61·8	43·9	60·4	45·5	64·9	46·9	48·7	45·1	36·8	41·9
Ni	75·9	50·8	50·2	33·8	75·7	88·8	73·6	91·2	85·7	63·4	75·3	75·9	66·7	57·9	83·6
Cu	61·2	61·4	51·9	71·3	118	96·6	95·1	111	95·7	109	124	131	130	107	104
Zn	109	103	107	88·4	95·2	96·5	98·6	141	106	143	73·2	84·7	73·1	54·0	59·5
Ga	20·0	20·4	19·8	20·0	19·3	19·8	19·6	22·4	19·0	22·7	16·8	17·5	16·5	16·0	15·9
Rb	11·7	11·6	11·7	38·9	6·17	3·65	18·4	18·0	75·1	13·8	0·948	1·15	1·10	1·10	1·22
Sr	223	228	213	207	211	220	223	308	224	315	125	124	133	145	147
Y	29·8	29·4	29·7	29·4	29·6	28·6	28·3	32·5	29·9	32·8	26·3	28·7	23·6	18·0	19·1
Zr	136	142	132	131	134	139	129	150	136	151	75·4	76·9	61·9	46·6	52·2
Nb	9·66	10·1	9·39	9·18	9·12	9·41	8·63	10·4	9·30	10·4	2·81	3·46	2·67	2·03	2·30
Ba	65·5	114	83·1	69·8	59·5	60·4	56·4	130	65·9	124	18·2	20·3	18·1	14·0	16·0
La	9·16	9·25	8·63	9·26	8·13	8·23	7·74	9·24	8·37	9·22	3·04	3·33	2·73	2·08	2·32
Ce	23·8	24·4	22·6	24·1	21·6	22·0	20·5	24·3	22·1	24·5	9·27	9·80	7·98	6·10	6·82
Pr	3·54	3·63	3·39	3·44	3·32	3·37	3·15	3·74	3·40	3·75	1·62	1·69	1·38	1·06	1·17
Nd	16·3	16·6	15·6	15·6	15·7	15·8	15·0	17·6	16·0	17·9	8·57	8·94	7·37	5·66	6·22
Sm	4·62	4·70	4·49	4·43	4·63	4·59	4·38	5·15	4·69	5·22	3·02	3·20	2·65	2·03	2·22
Eu	1·62	1·68	1·57	1·56	1·68	1·70	1·61	1·87	1·70	1·90	1·20	1·24	1·06	0·844	0·887
Tb	0·892	0·905	0·888	0·877	0·890	0·880	0·855	0·986	0·905	1·01	0·717	0·779	0·638	0·488	0·526
Gd	5·36	5·39	5·26	5·22	5·44	5·33	5·17	6·01	5·51	6·10	4·01	4·35	3·55	2·73	2·94
Dy	5·80	5·81	5·79	5·67	5·79	5·67	5·50	6·38	5·87	6·49	4·91	5·32	4·40	3·34	3·54
Ho	1·21	1·21	1·20	1·19	1·19	1·16	1·13	1·32	1·20	1·32	1·06	1·15	0·934	0·718	0·758
Er	3·40	3·35	3·34	3·34	3·26	3·22	3·13	3·61	3·28	3·58	2·99	3·28	2·67	2·06	2·17
Tm	0·510	0·494	0·494	0·500	0·476	0·461	0·457	0·528	0·484	0·524	0·455	0·487	0·400	0·307	0·318
Yb	3·20	3·08	3·12	3·11	2·96	2·90	2·85	3·28	3·01	3·26	2·88	3·13	2·54	1·94	2·05
Lu	0·475	0·450	0·460	0·470	0·444	0·425	0·419	0·476	0·444	0·479	0·429	0·463	0·381	0·292	0·300
Hf	3·55	3·66	3·43	3·39	3·54	3·60	3·39	3·96	3·52	4·03	2·17	2·27	1·83	1·39	1·51
Ta	0·609	0·643	0·592	0·576	0·583	0·589	0·545	0·649	0·577	0·650	0·181	0·226	0·172	0·135	0·147
Pb	1·12	1·25	0·915	0·399	0·550	0·780	0·705	0·793	0·803	1·10	1·90	0·411	0·516	0·122	0·482
Th	0·640	0·662	0·619	0·604	0·571	0·576	0·530	0·638	0·570	0·637	0·175	0·220	0·169	0·125	0·143
U	0·891	0·900	0·765	0·789	0·140	0·469	0·185	0·738	0·449	0·671	0·0623	0·158	0·0600	0·0440	0·0498

Table 2: continued

Sample:	55-9	55-10	55-11	55-12	55-13	55-14	55-15	55-16	55-5	55-6	55-7	55-8	55-1	55-2	55-3	55-4
Seamount:	Suiko	Suiko	Suiko	Suiko	Suiko	Suiko	Suiko	Suiko	Nintoku	Nintoku	Nintoku	Nintoku	Ojin	Ojin	Ojin	Ojin
Rock type:	AB	AB	AB	T	PB	T	T	T	H	AB	AB	AB	H	H	H	T
Stage:	PS	PS	PS	S	S	S	S	S	PS	PS	PS	PS	PS	PS	PS	S
SiO_2	47·79	46·73	46·91	48·14	45·51	49·63	48·74	46·86	47·68	47·05	46·67	47·11	49·51	49·51	50·05	48·39
TiO_2	3·22	3·19	2·94	2·62	1·25	2·56	2·80	2·70	2·74	2·65	3·13	2·98	2·93	2·87	2·88	2·88
Al_2O_3	14·23	14·04	13·81	13·96	9·23	14·24	14·03	14·41	19·86	16·35	18·61	15·65	15·68	16·00	16·02	14·86
Fe_2O_3	14·82	15·06	14·55	14·11	13·70	12·70	13·73	13·74	11·31	12·78	14·26	14·33	12·48	12·09	11·66	13·17
MnO	0·18	0·19	0·20	0·16	0·17	0·15	0·17	0·17	0·07	0·15	0·14	0·19	0·13	0·12	0·11	0·19
MgO	4·92	5·13	6·88	6·62	21·71	6·52	6·25	8·16	2·53	5·74	2·67	5·50	4·55	4·44	3·98	5·42
CaO	9·23	9·48	9·63	10·28	5·39	10·12	10·47	9·82	7·73	10·20	8·50	8·20	6·99	6·93	7·04	10·88
Na_2O	3·67	3·55	3·18	2·92	1·77	2·88	2·88	3·04	4·60	3·32	3·80	3·94	4·30	4·41	4·53	3·09
K_2O	0·99	0·91	0·81	0·29	0·91	0·24	0·23	0·42	1·50	0·94	1·41	1·16	1·56	1·63	1·69	0·39
P_2O_5	0·44	0·43	0·39	0·27	0·11	0·26	0·32	0·30	1·22	0·54	0·69	0·49	1·21	1·35	1·35	0·32
LOI	0·26	0·16	0·39	0·18	2·66	0·00	0·00	0·41	3·10	1·66	2·21	0·47	1·06	1·18	1·01	0·00
Total	99·51	98·71	99·32	99·37	99·76	99·30	99·61	99·66	99·24	99·73	99·89	99·56	99·34	99·36	99·31	99·57
Sc	28·3	28·3	27·6	31·6	19·4	30·6	30·1	25·0	9·47	18·9	20·6	17·5	14·0	13·2	13·2	26·2
Ti	17578	17334	15899	13992	6828	14505	14836	15552	15032	14954	17161	16360	17404	16671	16568	16329
V	325	321	314	288	151	273	272	240	84·4	218	257	188	156	140	141	271
Cr	47·1	44·1	181	74·7	864	146	141	221	1·57	92·2	99·0	76·7	0·724	0·404	0·327	84·1
Co	45·2	46·4	49·7	49·3	92·4	45·0	46·0	56·5	37·5	44·3	49·7	40·4	32·8	30·1	29·2	46·7
Ni	43·8	44·3	99·5	54·8	952	59·3	59·8	182	17·4	67·1	58·5	45·1	12·1	9·91	9·30	56·5
Cu	80·0	112	95·5	88·8	56·1	95·2	82·1	68·0	33·0	64·9	41·5	45·9	25·6	24·0	21·1	97·2
Zn	139	140	129	124	99·2	123	128	123	124	126	171	139	172	173	172	133
Ga	24·3	24·2	22·9	21·8	13·1	21·6	22·1	21·7	22·1	23·5	26·5	24·2	28·8	29·5	29·8	22·6
Rb	16·0	15·4	13·4	2·03	12·5	1·93	2·00	4·80	11·8	15·0	22·0	20·5	25·5	17·0	22·0	3·69
Sr	399	392	367	308	126	303	318	342	1040	619	668	521	633	664	677	409
Y	30·1	29·4	26·8	28·3	13·5	25·6	29·6	26·6	31·6	19·0	20·2	23·6	46·3	49·5	49·8	27·5
Zr	218	214	193	153	65·0	147	175	166	281	163	197	195	440	479	480	168
Nb	29·7	28·9	26·5	13·8	5·04	12·7	15·4	14·6	84·2	36·4	44·4	41·1	45·0	48·2	48·3	17·3
Ba	237	229	210	79·8	62·2	66·5	61·6	90·3	809	327	422	358	344	379	382	119
La	21·4	21·0	19·1	11·6	4·03	10·2	12·2	11·6	59·0	23·8	27·8	25·3	38·2	42·0	42·3	13·0
Ce	49·2	48·3	43·9	28·4	10·6	26·2	31·0	29·6	119	51·1	57·7	54·0	92·8	102	103	32·5
Pr	6·75	6·59	5·95	4·20	1·62	3·89	4·62	4·41	14·1	6·60	7·70	6·92	13·1	14·5	14·4	4·77
Nd	28·7	28·1	25·4	19·6	7·87	18·1	21·4	20·4	52·4	26·8	31·1	27·8	57·6	63·1	63·2	21·8
Sm	7·07	6·99	6·27	5·46	2·38	5·24	6·03	5·77	10·2	6·03	6·80	6·32	14·2	15·6	15·6	6·07
Eu	2·48	2·44	2·22	2·02	0·927	1·96	2·19	2·09	3·24	2·15	2·49	2·26	4·56	4·94	4·97	2·22
Tb	1·09	1·08	0·974	0·967	0·454	0·926	1·05	0·965	1·20	0·802	0·882	0·902	1·93	2·07	2·07	1·01
Gd	7·31	7·23	6·52	6·23	2·85	5·90	6·73	6·28	8·54	5·70	6·38	6·24	13·7	14·7	14·7	6·65
Dy	6·46	6·35	5·76	5·95	2·80	5·54	6·22	5·71	6·79	4·40	4·84	5·18	10·7	11·4	11·4	6·02
Ho	1·25	1·22	1·10	1·15	0·556	1·08	1·20	1·09	1·24	0·788	0·854	0·970	1·86	2·00	2·01	1·13
Er	3·13	3·07	2·77	3·01	1·46	2·75	3·10	2·81	3·12	1·89	2·05	2·42	4·43	4·75	4·79	2·83
Tm	0·424	0·422	0·380	0·415	0·202	0·375	0·424	0·372	0·426	0·242	0·260	0·319	0·579	0·619	0·618	0·384
Yb	2·52	2·47	2·22	2·42	1·19	2·24	2·53	2·24	2·53	1·39	1·49	1·90	3·25	3·48	3·51	2·21
Lu	0·237	0·361	0·324	0·351	0·174	0·321	0·356	0·317	0·358	0·196	0·204	0·275	0·452	0·479	0·485	0·306
Hf	5·41	5·32	4·76	3·99	1·76	3·92	4·58	4·30	6·17	3·92	4·70	4·62	10·4	11·2	11·3	4·42
Ta	1·76	1·73	1·58	0·858	0·323	0·802	0·945	0·916	4·77	2·16	2·62	2·43	2·63	2·83	2·83	1·05
Pb	2·77	1·70	1·46	1·24	0·376	1·29	1·43	7·45	3·81	2·20	1·86	1·76	3·23	3·04	2·78	1·41
Th	1·89	1·85	1·68	0·826	0·287	0·759	0·908	0·866	6·12	2·22	2·75	2·53	2·96	3·28	3·30	0·939
U	0·596	0·607	0·558	0·543	0·0653	0·263	0·311	0·286	1·79	0·690	0·951	0·824	1·08	0·979	1·06	0·349

Sample:	A43D-a	A43D-c	A43D-d	A43D-g	A44D-a	A44D-b	A44D-c	A51D-a	A53D-b	A53D-c	A55D-b	A55D-d	A55D-e	BHVO-1	%RSD
Seamount:	Koko	Koko	Koko	Koko	Koko	Koko	Koko	Kimmei	Yuryaku	Yuryaku	Daikakuji	Daikakuji	Daikakuji	Av. (n = 82)	
Rock type:	T	M	Tr	Tr	TB	TB	AB	AB	AB	T	TB?	AB?		TB?	
Stage:	S	PS	PS	PS	PS?	PS?	PS	PS	PS	S?	PS?	PS?	PS?		
SiO_2	49·27	48·59	61·64	61·47	48·80	48·54	47·75	45·62	47·29	48·42	50·62	48·38	51·79		
TiO_2	2·70	1·97	0·02	0·02	3·66	3·69	3·70	3·40	3·93	3·14	3·27	3·18	2·96		
Al_2O_3	14·07	16·65	19·59	19·50	13·34	13·25	13·41	15·81	18·43	14·96	14·41	14·37	13·40		
Fe_2O_3	13·20	14·17	3·56	3·66	14·68	14·63	15·02	13·62	13·99	12·09	12·83	11·79	10·91		
MnO	0·17	0·20	0·18	0·22	0·17	0·18	0·18	0·47	0·09	0·11	0·14	0·16	0·13		
MgO	6·19	2·38	0·07	0·15	4·93	4·92	5·07	3·86	3·83	6·56	4·47	6·13	6·50		
CaO	10·49	5·17	0·43	0·47	9·93	9·97	10·15	11·14	6·34	9·92	8·56	10·56	8·90		
Na_2O	2·80	5·34	9·05	9·24	2·92	3·08	2·92	3·30	3·85	3·22	3·36	3·17	3·26		
K_2O	0·63	2·65	5·51	4·93	0·86	0·69	0·83	0·87	1·58	0·67	1·39	0·84	1·24		
P_2O_5	0·29	2·30	0·01	0·01	0·51	0·51	0·58	1·56	0·44	0·29	0·63	1·21	0·55		
LOI	0·07	1·97	3·21	1·60	0·37	0·21	0·51	1·75	2·10	0·83	0·59	1·67	0·27		
Total	99·85	99·42	100·06	99·67	99·81	99·48	99·63	99·65	99·81	99·42	99·69	99·83	99·68		
Sc	30·6	5·41	5·01	2·43	30·7	30·5	30·6	25·1	33·0	31·1	20·0	22·4	19·9	29·9	1·68
Ti	16155	11692	62	83	22184	21891	21775	19400	22652	18195	18622	17831	16191	16376	1·02
V	290	35·3	1·78	1·01	330	330	333	268	313	261	238	228	203	286	1·39
Cr	246	0·361	0·040	0·010	78·4	78·1	79·3	218	269	262	49·6	267	218	295	2·37
Co	47·4	29·2	0·752	0·201	44·7	49·6	41·2	149	50·0	47·6	37·2	48·7	42·7	46·7	1·53
Ni	92·8	51·3	2·73	0·764	50·2	56·9	43·6	136	144	93·5	61·1	174	183	117	2·57
Cu	96·7	21·1	4·46	4·25	85·0	83·4	77·4	80·4	70·2	54·2	52·2	77·9	77·7	137	0·94
Zn	132	247	443	545	150	152	159	178	150	155	155	223	124	106	1·81
Ga	21·5	26·1	74·8	78·0	23·2	23·2	23·1	25·3	27·7	22·1	24·0	22·4	21·4	21·2	1·18
Rb	9·71	42·4	196	210	18·5	14·3	22·0	16·9	18·9	9·40	26·7	11·6	19·4	9·27	0·83
Sr	310	2152	17·5	39·7	358	360	355	513	448	383	599	688	598	394	0·52
Y	26·4	52·6	138	162	33·9	34·1	35·9	37·5	13·4	22·8	33·4	32·3	26·0	22·9	0·76
Zr	153	604	1501	1699	202	204	205	239	210	160	276	288	259	165	0·94
Nb	12·5	77·8	228	255	23·0	23·2	23·2	23·8	21·7	16·3	28·5	28·0	25·4	18·5	0·86
Ba	80·3	842	11·2	9·04	141	149	94·7	200	149	91·1	295	238	319	132	0·75
La	10·3	86·7	141	166	17·3	17·4	18·2	22·3	14·3	11·5	26·6	29·5	24·5	15·1	0·74
Ce	25·9	206	325	377	42·2	42·6	43·0	47·6	31·4	27·5	60·6	61·4	55·0	37·7	0·65
Pr	4·04	28·4	39·4	45·5	6·19	6·23	6·36	6·82	4·63	4·15	8·31	8·44	7·43	5·46	0·55
Nd	19·0	118	139	159	28·0	28·1	28·6	30·0	19·7	19·1	35·5	35·8	31·6	24·1	0·52
Sm	5·57	24·6	29·7	34·0	7·56	7·60	7·66	7·88	4·83	5·50	8·94	8·77	7·74	5·95	0·79
Eu	1·98	8·19	2·27	2·56	2·61	2·63	2·66	2·72	2·13	2·09	3·05	2·94	2·63	2·04	0·98
Tb	0·955	2·64	2·57	5·32	1·26	1·26	1·29	1·26	0·649	0·933	1·33	1·22	1·09	0·886	0·97
Gd	6·09	20·3	26·6	30·6	8·13	8·12	8·26	8·34	4·61	5·99	8·96	8·46	7·50	5·97	0·68
Dy	5·61	13·3	27·8	32·3	7·34	7·38	7·54	7·27	3·40	5·27	7·44	6·75	6·02	5·12	0·85
Ho	1·08	2·22	5·33	6·22	1·43	1·43	1·46	1·40	0·600	0·981	1·37	1·24	1·09	0·954	0·84
Er	2·73	4·95	14·2	16·3	3·57	3·57	3·69	3·42	1·40	2·36	3·37	2·98	2·61	2·42	1·32
Tm	0·371	0·586	2·03	2·33	0·490	0·489	0·500	0·457	0·182	0·308	0·439	0·391	0·341	0·324	1·28
Yb	2·19	3·27	12·1	13·7	2·90	2·92	2·99	2·71	1·09	1·81	2·58	2·28	1·96	1·90	1·05
Lu	0·310	0·445	1·65	1·86	0·411	0·415	0·424	0·389	0·152	0·245	0·360	0·323	0·274	0·268	1·36
Hf	4·02	12·9	44·5	49·6	5·18	5·21	5·25	6·10	5·50	4·28	6·83	6·89	6·22	4·37	1·28
Ta	0·793	4·57	17·4	19·5	1·45	1·45	1·48	1·48	1·35	1·01	1·73	1·75	1·53	1·15	1·31
Pb	0·713	3·72	20·8	23·8	1·15	1·12	1·53	2·04	1·25	0·972	1·92	2·27	1·82	1·97	3·87
Th	0·696	5·06	27·7	32·4	1·34	1·33	1·34	1·96	1·35	0·951	2·47	2·48	2·21	1·19	1·09
U	0·301	1·87	6·50	10·1	0·486	0·480	0·481	1·22	0·650	0·202	0·688	1·16	0·668	0·433	1·09

Major element concentrations in wt %; trace element concentrations in ppm. LOI, loss on ignition. All concentrations have been recalculated on a volatile-free basis. PB, picrite basalt; AB, alkali basalt; T, tholeiite; TB, transitional basalt; H, hawaiite; M, mugearite; Tr, trachyte. Samples are classified into shield (S) and post-shield (PS) lavas on the basis of SiO_2–(Na_2O + K_2O) and P_2O_5–TiO_2 relationships.

Sr, Nd and Pb isotope analyses were carried out at the Max-Planck-Institut für Chemie, Mainz. Before dissolution, sample powders for Sr and Pb isotope analysis were subjected to an acid leaching procedure to remove alteration products. Approximately 4–5 g of rock powder was weighed into a Teflon beaker, and 5–10 ml once-distilled 6M HCl added. The samples were placed in an ultrasonic bath for 2 h; the acid was changed every 20 min. The samples were then leached in hot (~80°C) 6M HCl for a further 5 h; the acid was changed every 60 min. The residue was soaked in deionized water at 80°C for 30 min, rinsed twice, and dried. The weight loss as a result of leaching was between 55 and 71%. Microscopic examination of the residue showed that the leaching procedure leaves a residue of plagioclase, clinopyroxene, ± olivine and opaque minerals. Rb and Sr concentrations in the leached powders were determined by isotope dilution, and U, Th and Pb concentrations were measured by ICP-MS.

The leached sample powder (100–200 mg) was digested in HF–HNO_3 for Pb isotope analysis, and Pb was separated from the sample matrix by anion exchange in HNO_3–HBr mixtures, as described by Lugmair & Galer (1992). Rb and Sr were separated using conventional cation exchange techniques from a separate dissolution of leached sample powder. Nd isotope analyses were carried out on unleached powders. The rare earth elements (REE) were separated from the sample matrix using standard cation exchange procedures, and Nd was then separated from the other REE by cation exchange using α-hydroxyisobutyric acid as eluant. Total procedural blanks were below 500, 80 and 60 pg for Sr, Nd and Pb, respectively.

Isotope analyses were carried out in static multicollection mode using a Finnigan MAT-261 mass spectrometer. Sr and Nd isotope ratios were corrected for fractionation using $^{86}Sr/^{88}Sr = 0{\cdot}1194$ and $^{146}Nd/^{144}Nd = 0{\cdot}7219$. The NBS-987 Sr and La Jolla Nd standards gave $^{87}Sr/^{86}Sr = 0{\cdot}710223 \pm 18$ and $^{143}Nd/^{144}Nd = 0{\cdot}511872 \pm 10$ (2σ), respectively, during the period of analysis. Sr and Nd isotope data in Table 3 have been normalized to values of 0·710245 and 0·511855 for these standards. Pb isotope analyses were carried out using a triple-spike technique to correct for instrumental mass fractionation (Galer, 1999). After elution of the Pb fraction from the ion exchange columns, 5–10% was transferred to a second beaker, and spiked with an optimal amount of ^{204}Pb–^{206}Pb–^{207}Pb triple spike. The spiked and unspiked Pb fractions were measured separately on the mass spectrometer, and the data were then combined to obtain the fractionation-corrected Pb isotope composition of the sample (Galer, 1999). During this study, the NBS-981 Pb standard gave $^{206}Pb/^{204}Pb$ $16{\cdot}9403 \pm 22$, $^{207}Pb/^{204}Pb$ $15{\cdot}4974 \pm 20$, $^{208}Pb/^{204}Pb$ $36{\cdot}7246 \pm 58$ (2σ, $n = 19$).

EFFECTS OF LEACHING AND AGE CORRECTION ON THE ISOTOPE DATA

Few of the samples analysed have both Ce/Pb and Nb/U ratios within the range of fresh oceanic lavas (Hofmann *et al.*, 1986), indicating that alteration has modified the U and Pb concentrations of many of the lavas since crystallization. Pb and Sr isotope analyses were therefore carried out on leached sample powders, in an attempt to obtain meaningful Sr and Pb isotope data from samples that gained or lost Rb, Sr, U and Pb during subsolidus alteration.

The leaching procedure we used is similar to that of previous studies, and has been shown to be effective at removing alteration products from altered basaltic rocks (Cheng *et al.*, 1987; Mahoney, 1987). Experiments carried out in this study showed that more intense leaching did not lead to a significant further decrease in initial $^{87}Sr/^{86}Sr$ ratios (Table 3). Compared with the unleached rock powder, the leached residues generally have significantly lower Rb concentrations, and similar or higher Sr contents (Tables 2 and 3). These changes are probably the result of removal of clay minerals and concentration of plagioclase in the residue during leaching.

Seawater has an extremely low Pb concentration, and so if alteration changes U/Pb soon after eruption, reliable initial Pb isotope ratios could be obtained from unleached powders (Staudigel *et al.*, 1995). However, recent studies have shown that this is often not the case (Mahoney *et al.*, 1998). We analysed unleached powders of three samples. Two of these (19-1 and 145-10) yielded very different initial Pb isotope compositions from those of the corresponding leached powders, whereas initial Pb isotope ratios of leached and unleached aliquots of sample 145-11 were very similar (Table 4). Leached and unleached samples do not differ in any systematic way (Table 4). As a result of the low U/Pb, Th/Pb ratios in plagioclase, measured Pb isotope ratios in this mineral should be close to the whole-rock initial value. A plagioclase separate from sample 145-11 yielded similar Pb isotope ratios to the age-corrected leached whole-rock powder (Table 4). These results suggest that accurate Pb isotope data for old, altered basaltic rocks may be obtained from leached rock powders. We therefore carried out Pb isotopic measurements on leached sample powders. U, Th and Pb concentrations are all significantly lower in the leached powders than in the unleached samples (Table 4).

The measured Ce and Nb concentrations of the samples could be used to estimate their Pb and U

Table 3: Sr and Nd isotope data for Emperor-Hawaiian Seamount lavas

Sample	Seamount	Stage	Rb	Sr	$^{87}Sr/^{86}Sr$ (measured)	$^{87}Sr/^{86}Sr$ (initial)	ε_{Sr}	Sm	Nd	$^{143}Nd/^{144}Nd$ (measured)	$^{143}Nd/^{144}Nd$ (initial)	ε_{Nd}
19-1	Meiji	S	3·47	178	0·702992	0·702924	−21·0	4·62	16·3	0·513038	0·512943	8·08
19-2	Meiji	S	6·51	229	0·703205	0·703106	−18·4	4·70	16·6	0·512997	0·512902	7·29
19-3	Meiji	S	7·75	212	0·703319	0·703191	−17·2	4·49	15·6	0·513022	0·512926	7·75
19-4	Meiji	S	9·75	215	0·703331	0·703172	−17·4	4·43	15·6	0·513051	0·512956	8·34
19-4*	Meiji	S						1·04	2·63	0·513064	0·512967	8·55
145-1	Detroit	PS?	3·05	214	0·702828	0·702781	−23·1	4·63	15·7	0·513063	0·512969	8·49
145-2	Detroit	PS?	2·94	223	0·702827	0·702783	−23·0	4·59	15·8	0·513068	0·512976	8·62
145-3	Detroit	PS?	3·56	203	0·702871	0·702813	−22·6	4·38	15·0	0·513075	0·512982	8·73
145-4	Detroit	PS?	4·64	363	0·702801	0·702759	−23·4	5·15	17·6	0·513086	0·512993	8·96
145-7	Detroit	S	0·199	106	0·702638	0·702632	−25·2	3·02	8·57	0·513158	0·513046	9·99
145-8	Detroit	S	0·222	112	0·702763	0·702756	−23·4	3·20	8·94	0·513151	0·513037	9·81
145-9	Detroit	S	0·258	103	0·702693	0·702685	−24·4	2·65	7·37	0·513187	0·513072	10·51
145-10	Detroit	S	0·284	98·9	0·702677	0·702667	−24·7	2·03	5·66	0·513141	0·513027	9·61
145-11	Detroit	S	0·283	96·6	0·702642	0·702632	−25·2	2·22	6·22	0·513147	0·513033	9·74
55-9	Suiko	PS	12·7	431	0·703128	0·703053	−19·5	7·07	28·7	0·513006	0·512946	7·56
55-10	Suiko	PS	13·5	439	0·703097	0·703018	−20·0	6·99	28·1	0·513006	0·512945	7·55
55-10	(10 h leach)		13·6	391	0·703119	0·703030	−19·8					
55-10	(12 h leach)		14·2	415	0·703139	0·703052	−19·5					
55-10	(24 h leach)		14·5	393	0·703143	0·703049	−19·6					
55-12	Suiko	S	0·573	336	0·703244	0·703240	−16·9	5·46	19·6	0·513047	0·512979	8·21
55-13	Suiko	S	0·183	82·6	0·703290	0·703284	−16·2	2·38	7·87	0·513031	0·512957	7·79
55-14	Suiko	S	1·59	302	0·703269	0·703256	−16·6	5·24	18·1	0·513024	0·512953	7·71
55-14*	Suiko	S						1·56	3·94	0·513057	0·512960	7·84
55-15	Suiko	S	0·289	304	0·703240	0·703238	−16·9	6·03	21·4	0·513003	0·512934	7·34
55-15*	Suiko	S						1·56	3·64	0·513083	0·512978	8·20
55-16	Suiko	S	4·24	350	0·703330	0·703299	−16·0	5·77	20·4	0·513005	0·512936	7·37
55-5	Nintoku	PS	7·20	1540	0·703111	0·703100	−18·9	10·2	52·4	0·512999	0·512956	7·62
55-5†	Nintoku	PS	7·20	1540	0·703115	0·703104	−18·9					
55-6	Nintoku	PS	12·4	649	0·703203	0·703159	−18·1	6·03	26·8	0·513016	0·512966	7·81
55-6†	Nintoku	PS	12·4	649	0·703206	0·703162	−18·1					
55-8	Nintoku	PS	18·5	649	0·703203	0·703137	−18·4	6·32	27·8	0·513022	0·512972	7·92
55-1	Ojin	PS	25·8	712	0·703523	0·703441	−14·1	14·2	57·6	0·513007	0·512953	7·54
55-2	Ojin	PS	18·4	744	0·703486	0·703430	−14·3	15·6	63·1	0·513042	0·512988	8·22
55-3	Ojin	PS	23·3	772	0·703480	0·703412	−14·5	15·6	63·2	0·513038	0·512984	8·15
55-4	Ojin	S	2·66	334	0·703404	0·703386	−14·9	6·07	21·8	0·513030	0·512970	7·85
A43D-a	Koko	S	3·26	253	0·703489	0·703464	−13·9	5·57	19·0	0·513044	0·512989	8·05
A44D-a	Koko	PS?	6·15	372	0·703353	0·703320	−16·0	7·56	28·0	0·513043	0·512992	8·11
A44D-b	Koko	PS?	4·78	382	0·703365	0·703340	−15·7	7·60	28·1	0·513051	0·513000	8·26
A51D-a	Kimmei	PS	1·42	616	0·703477	0·703473	−13·9	7·88	30·0	0·512985	0·512944	6·96
A53D-b	Yuryaku	PS	7·15	530	0·703471	0·703447	−14·2	4·83	19·7	0·513018	0·512976	7·69
A53D-c	Yuryaku	S	2·51	421	0·703476	0·703465	−14·0	5·50	19·1	0·513073	0·513024	8·62
A55D-b	Daikakuji	PS?	16·3	617	0·703744	0·703698	−10·7	8·94	35·5	0·512951	0·512909	6·35
A55D-e	Daikakuji	PS?	18·7	653	0·703827	0·703777	−9·56	7·74	31·6	0·512913	0·512872	5·63

Rb and Sr concentrations (in ppm) of leached sample powders were measured by isotope dilution. Except where stated otherwise, Sr isotope measurements were carried out on leached sample powders, and Nd isotope measurements on unleached powders. Sm and Nd concentrations (in ppm) of leached and unleached sample powders were measured by ICP-MS. ε_{Sr} and ε_{Nd} (relative to CHUR; present-day $^{143}Nd/^{144}Nd = 0{\cdot}512638$, $^{147}Sm/^{144}Nd = 0{\cdot}1967$) calculated from initial ratios. S, shield stage; PS, post-shield stage lavas.
*Repeat Nd isotope analysis of leached sample powder.
†Repeat Sr isotope analysis of a separate dissolution.

Table 4: Pb isotope compositions, and U, Th and Pb concentrations of Emperor Seamount lavas

Sample	$^{206}Pb/^{204}Pb$ (measured)	$^{207}Pb/^{204}Pb$ (measured)	$^{208}Pb/^{204}Pb$ (measured)	Pb	Th	U	U/Pb	Th/Pb	$^{206}Pb/^{204}Pb$ (initial)	$^{207}Pb/^{204}Pb$ (initial)	$^{208}Pb/^{204}Pb$ (initial)
19-1	18·9061 ± 14	15·4955 ± 16	38·0480 ± 49	0·125	0·0720	0·164	1·31	0·576	17·8048	15·4430	37·8890
19-1(u)	18·6392 ± 10	15·4777 ± 10	37·9191 ± 31	1·09	0·624	0·869	0·797	0·573	17·9716	15·4458	37·7619
19-2	18·7909 ± 19	15·4724 ± 19	38·0003 ± 56	0·149	0·129	0·161	1·081	0·866	17·8818	15·4291	37·7624
19-3	18·9332 ± 20	15·4837 ± 23	38·0756 ± 72	0·142	0·139	0·183	1·29	0·979	17·8477	15·4319	37·8051
19-4	19·2160 ± 16	15·4979 ± 18	38·1359 ± 56	0·140	0·140	0·279	1·99	1·00	17·5255	15·4172	37·8583
145-1	18·1960 ± 21	15·4324 ± 22	37·8147 ± 65	0·180	0·0611	0·0261	0·145	0·339	18·0810	15·4269	37·7265
145-2	18·3972 ± 10	15·4561 ± 11	37·8381 ± 33	0·196	0·0579	0·145	0·740	0·295	17·8097	15·4281	37·7610
145-3	18·2741 ± 12	15·4509 ± 13	37·9619 ± 42	0·130	0·0540	0·0198	0·152	0·415	18·1526	15·4451	37·8533
145-10	18·1938 ± 17	15·4334 ± 18	37·7496 ± 52	0·0525	0·0456	0·0187	0·356	0·869	17·9118	15·4200	37·5241
145-10(u)	18·1268 ± 19	15·4590 ± 19	37·7406 ± 58	0·121	0·124	0·0437	0·361	1·03	17·8422	15·4454	37·4748
145-11	18·1041 ± 14	15·4321 ± 15	37·6704 ± 44	0·103	0·0364	0·0165	0·160	0·353	17·9775	15·4261	37·5789
145-11(u)	18·0825 ± 11	15·4319 ± 10	37·6590 ± 31	0·479	0·142	0·0495	0·104	0·297	18·0009	15·4280	37·5823
145-11(p)	18·057 ± 9	15·420 ± 9	37·600 ± 20								
55-9	18·3858 ± 11	15·4592 ± 11	37·9323 ± 34	0·900	0·539	0·306	0·340	0·599	18·1788	15·4494	37·8124
55-12	18·5276 ± 10	15·4609 ± 10	37·9757 ± 31	0·390	0·0957	0·0698	0·179	0·245	18·4182	15·4558	37·9263
55-14	18·5850 ± 11	15·4701 ± 11	38·1182 ± 33	0·427	0·295	0·137	0·321	0·691	18·3891	15·4603	37·9793
55-15	18·6033 ± 15	15·4759 ± 15	38·1266 ± 45	0·152	0·0326	0·0265	0·174	0·215	18·4965	15·4708	38·0834
55-16	18·6057 ± 10	15·4691 ± 10	38·1380 ± 30	0·580	0·410	0·193	0·333	0·707	18·4021	15·4595	37·9955
55-5	18·1785 ± 14	15·4564 ± 16	37·7569 ± 51	0·935	0·0358	0·0507	0·054	0·0383	18·1487	15·4550	37·7500
55-5(r)	18·1805 ± 14	15·4575 ± 16	37·7600 ± 49	0·935	0·0358	0·0507	0·054	0·0383	18·1507	15·4561	37·7531
55-6	18·2474 ± 13	15·4537 ± 14	37·8219 ± 41	0·470	0·270	0·118	0·251	0·575	18·1104	15·4472	37·7185
55-1	18·4366 ± 12	15·4680 ± 12	37·9298 ± 36	1·93	1·36	0·678	0·351	0·705	18·2468	15·4591	37·8051
55-2	18·4227 ± 8	15·4669 ± 8	37·9497 ± 24	1·59	1·16	0·627	0·394	0·730	18·2090	15·4568	37·8194
55-3	18·4420 ± 10	15·4713 ± 10	37·9634 ± 28	1·59	1·25	0·716	0·450	0·786	18·1981	15·4598	37·8241
55-4	18·4639 ± 10	15·4693 ± 11	37·9921 ± 32	0·468	0·331	0·145	0·310	0·707	18·2959	15·4613	37·8661
A43D-a	18·4600 ± 10	15·4705 ± 10	37·9666 ± 31	0·280	0·165	0·0944	0·337	0·589	18·3008	15·4631	37·8751
A44D-a	18·4781 ± 15	15·4742 ± 13	38·0236 ± 37	0·609	0·348	0·155	0·255	0·571	18·3579	15·4686	37·9349
A53D-c	18·4218 ± 9	15·4624 ± 9	37·9874 ± 29	0·552	0·0938	0·0656	0·119	0·170	18·3712	15·4600	37·9636
A55D-b	18·2281 ± 11	15·4531 ± 11	38·0366 ± 33	1·42	1·12	0·390	0·275	0·789	18·1142	15·4478	37·9291
A55D-e	18·0811 ± 10	15·4302 ± 11	37·9654 ± 34	1·75	1·51	0·490	0·280	0·863	17·9652	15·4248	37·8478

Except where indicated, all analyses were carried out on leached sample powders. Initial Pb isotope ratios were calculated using the age of each seamount given in Table 1. U, Th and Pb concentrations (in ppm) were measured by ICP-MS. (u), unleached sample; (r), repeat analysis of a separate dissolution; (p), plagioclase separate.

concentrations before alteration, assuming that the rocks had Ce/Pb and Nb/U ratios typical of other oceanic basalts before alteration. However, U/Pb ratios calculated in this way can be used for age correction only if the alteration occurred recently, but many samples contain petrographic evidence for multiple alteration events (e.g. zoning of secondary minerals infilling vesicles). In addition, Ce/Pb ratios of many of the samples are lower than those typical of most oceanic basalts, indicating that they have gained Pb, probably from seawater, during the alteration process.

Although moderate degrees of sea-floor alteration have no significant effect upon Nd isotope compositions of basalts (e.g. Staudigel *et al.*, 1995), the Fe–Mn coatings on some of the samples are potentially a source of Nd (and Pb) contamination. Samples for isotope measurements were therefore carefully handpicked to avoid these coatings. We carried out Nd isotope analyses on three samples that had been subjected to the leaching procedure. Of these, two samples yielded initial $^{143}Nd/^{144}Nd$ ratios within error of those of the unleached powders (despite a large decrease in Sm and Nd concentrations; see Table 3), whereas the other leached sample had a somewhat higher initial $^{143}Nd/^{144}Nd$ ratio than that of the unleached powder. As the leaching procedure would have removed any Fe–Mn coating present (Cheng *et al.* 1987), we conclude that alteration has not significantly modified the Nd isotope ratios of the unleached samples.

Measured Sr, Nd and Pb isotope ratios were corrected for radioactive decay since eruption using the known age of each seamount (Table 1). A potential problem with age-correcting isotope data for leached samples is that the leaching procedure may have altered the parent/daughter ratios of the primary minerals left in the residue or preferentially removed radiogenic nuclides from damaged sites in the crystal structure. However, the fact that aliquots of the sample 55-10 that were leached for 10, 12 and 24 h (69–75% weight loss) yielded initial $^{87}Sr/^{86}Sr$ ratios similar to those of the same sample subjected to the usual 7 h procedure (61% weight loss) suggests that reliable initial Sr isotope ratios can be obtained from leached powders (see Table 3). A plagioclase separate from sample 145-11 yielded measured Pb isotope ratios very similar to the initial ratios calculated for the leached whole-rock sample (Table 4). As the measured Pb isotope compositions of plagioclase should be close to the initial ratio of the whole rock, we believe that the initial Pb isotope ratios calculated for the leached rock powders are also reliable.

RESULTS

Major and trace element composition

New major and trace element data for Emperor Seamount lavas are given in Table 2. Alteration has modified the compositions of most of the samples analysed, particularly the dredged samples. As a result, concentrations of mobile trace elements in many of the samples cannot be considered as primary. We have reported Rb, Sr, U and Pb concentrations in Table 2, to show the effects of leaching. Post-eruptive growth of secondary minerals (particularly calcite and clays) in vesicles, together with variable replacement of glass, olivine and plagioclase by alteration products such as smectite, calcite and Fe-oxyhydroxides, will have affected the concentrations of some major elements such as Ca, K, Na and P, given the observed abundance of these secondary minerals in the most altered samples. A rough estimate of the degree of alteration of the samples based on their petrography is included in Table 1.

Meiji Seamount (~ 85 Ma)

The four samples analysed from DSDP Site 192 are highly altered plagioclase ± clinopyroxene-phyric basalts, with MgO contents of between 5·8 and 6·9%. On an alkali–silica diagram (Fig. 2a), three of the samples plot within the field of alkalic basalts as a result of their high K_2O contents (Fig. 2f). However, Na_2O concentrations of the Meiji lavas are similar to those of other Emperor tholeiites, and the relatively high K_2O concentrations are probably the result of post-eruption alteration. In the TiO_2–P_2O_5 classification diagram (Fig. 2b), the samples plot within the field of ocean island tholeiites. The Meiji Seamount lavas have lower concentrations of TiO_2 and P_2O_5 than tholeiites from Suiko and younger seamounts (Fig. 2b).

The Meiji tholeiites have lower concentrations of the highly incompatible trace elements than many young tholeiitic basalts from the Hawaiian Islands with similar MgO. Concentrations of Th and Nb lie at the depleted end of the range of Hawaiian lavas (Fig. 3), and are similar to those of shield-building lavas from Mauna Loa (Hofmann & Jochum, 1996) and Koolau (Frey *et al.*, 1994). However, concentrations of the heavy rare earth elements (HREE) in the Meiji lavas are higher than those of young Hawaiian lavas (Fig. 4a), and La/Yb ratios are intermediate between those of tholeiites from the Hawaiian Islands and mid-ocean ridge basalt (MORB) from the East Pacific Rise (EPR) (Fig. 3).

Detroit Seamount (81·0 Ma)

The five flows sampled from Hole 884E are tholeiitic basalts containing 6·2–8·5% MgO. Samples 145-9, 145-10 and 145-11 contain up to 30% plagioclase phenocrysts, which may account for their higher CaO and Al_2O_3 contents compared with those of the other Emperor lavas. The Detroit tholeiites have lower TiO_2, P_2O_5 and K_2O, compared with other Hawaiian–Emperor tholeiites, which cannot be explained simply by the diluting effect

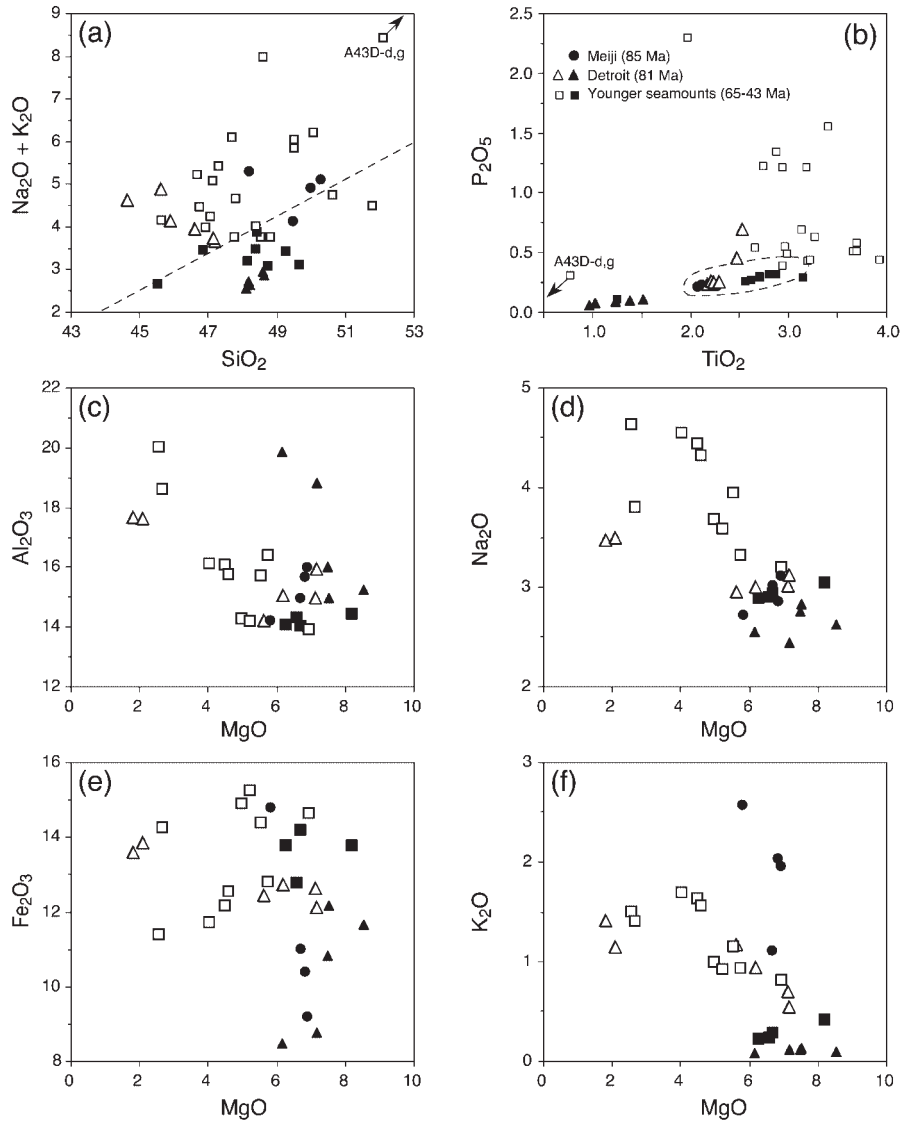

Fig. 2. Major element compositions of Emperor Seamount lavas. (a) and (b) show all data (drilled and dredged samples), and (c)–(f) show data for drilled samples only. Field in (b) shows range in TiO_2 and P_2O_5 for ocean island tholeiites (Garcia *et al.*, 1987). Filled symbols for tholeiitic lavas; open symbols for alkalic and transitional lavas. The low TiO_2, K_2O and P_2O_5 contents of the Detroit tholeiites compared with other Emperor lavas should be noted.

of plagioclase, as both TiO_2 and P_2O_5 are a factor of 2–3 lower than in most Hawaiian–Emperor lavas (Fig. 2b), and are also low in the aphyric samples 145-7 and 145-8.

Compared with tholeiites from the Hawaiian Islands, the Detroit tholeiites have lower concentrations of the highly incompatible trace elements (Figs 3 and 4b). Concentrations of the most incompatible elements such as Th are about seven times lower than in average Kilauea tholeiites for a given MgO value (Fig. 4), and are similar to the Th concentrations in Pacific N-type MORB (Fig. 3). The concentrations of the HREE (Er to Lu) are slightly higher in the Detroit tholeiites than in young Hawaiian tholeiites. Incompatible trace element patterns are similar to those of Pacific N-MORB (Fig. 4). The trace element compositions of the Detroit tholeiites are unlike those of most other intra-plate tholeiites, except the highly depleted lavas from the Galapagos Islands (White *et al.*, 1993).

The six samples from Site 883 are highly altered, plagioclase- and olivine-phyric lavas containing 1·8–7·2% MgO. Samples 145-4 and 145-6 have 1·8–2·0% MgO and are from different flows in Hole 883F. Keller *et al.* (1995) classified the Site 883 lavas as transitional between

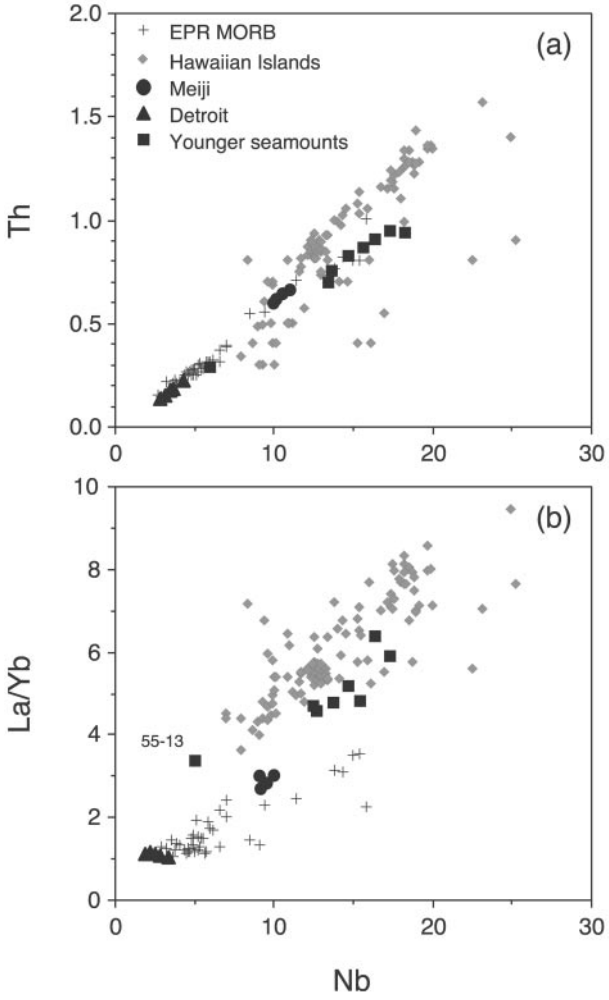

Fig. 3. Variation of (a) Th, and (b) La/Yb with Nb concentration in Emperor Seamount tholeiites. Data for N- and E-MORB from the northern EPR (Niu *et al.*, 1999; Regelous *et al.*, 1999) and for young Hawaiian tholeiitic basalts from Loihi, Kilauea, Mauna Loa, Mauna Kea, Kohala, Koolau and Kahoolawe (GEOROC geochemical database: http://georoc.mpch-mainz.gwdg.de) are shown for comparison.

tholeiitic and alkalic. On a total alkali–silica diagram (Fig. 2), the lavas plot above the alkali–tholeiite dividing line. However, compared with alkalic lavas from other Emperor Seamounts, the Site 883 lavas have lower P_2O_5, TiO_2 and Na_2O, and fall within the tholeiitic field in Fig. 2b.

The Site 883 lavas have higher concentrations of incompatible elements, and higher ratios of more- to less-incompatible elements compared with the tholeiites from Site 884 (Fig. 3). Concentrations of all elements more incompatible than Zr are lower than in young tholeiitic lavas from Kilauea (Fig. 4), and far lower than in Hawaiian alkalic or transitional basalts with similar MgO. Incompatible trace element compositions of the Site 883 lavas are similar to those of the Meiji tholeiites.

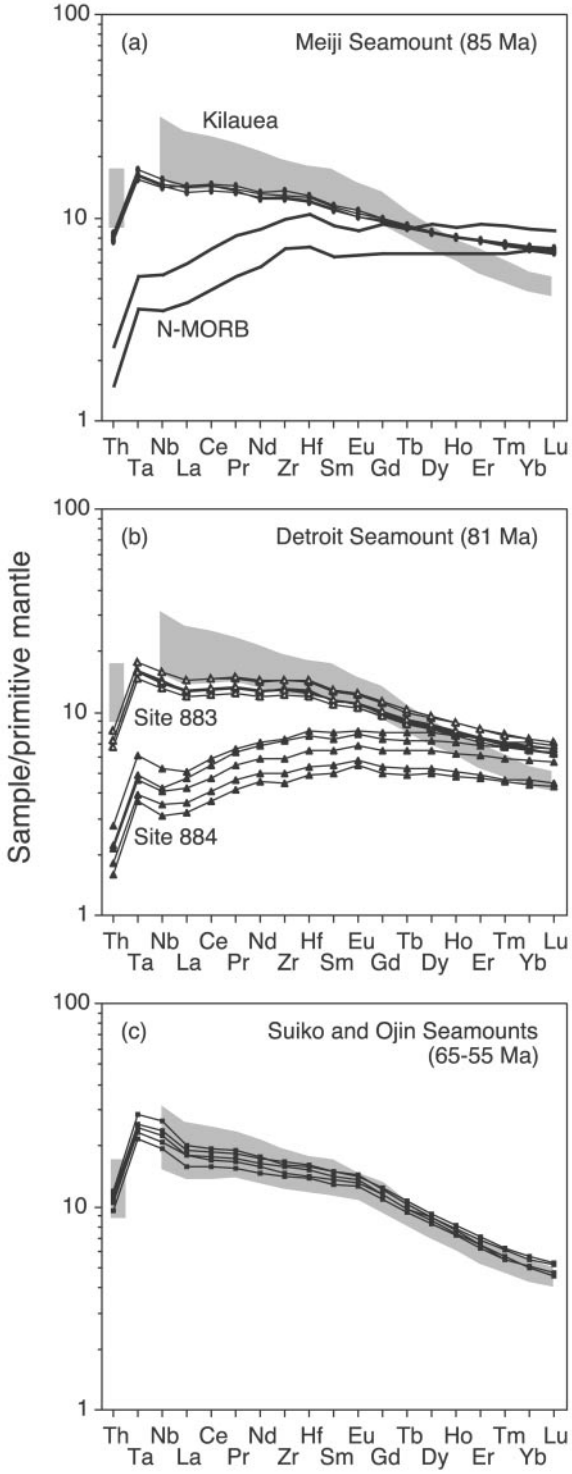

Fig. 4. Incompatible trace element concentrations of Emperor Seamount tholeiitic lavas (with MgO between 4·5 and 9·0%), normalized to the primitive mantle composition of McDonough & Sun (1995). Shaded field represents historical tholeiitic basalts from Kilauea summit volcano (Pietruszka & Garcia, 1999). The bold black lines in (a) represent average N-MORB estimates of Hofmann (1988) and Sun & McDonough (1989) (upper and lower curves, respectively).

However, compared with the latter, the Detroit lavas have lower SiO_2 for a given MgO, and in this respect are similar to young alkalic lavas from the Hawaiian Islands.

Younger seamounts (62–42 Ma)

Tholeiitic basalts were recovered from Suiko, Ojin, Koko, Yuryaku and Daikakuji Seamounts. One tholeiitic lava from Suiko Seamount (sample 55-13) has a picritic composition and contains cumulate olivine. Sample A55D-e, from Daikakuji, is a basaltic andesite. Alkali basalts occur on Suiko, Nintoku, Kimmei, Yuraku and Daikakuji Seamounts. Two phonolites (samples A43D-d and A43D-g) were dredged from the SE flank of Koko Seamount. Other samples from these seamounts include basalts of intermediate composition, hawaiites and a mugearite, all of which have similar major element compositions to lavas erupted during the post-shield volcanic stage on the Hawaiian Islands. Immobile trace element abundances of both tholeiitic and alkalic lavas from these seven seamounts are similar to those of equivalent rock types from the Hawaiian Islands (Figs 3 and 4, Table 2).

Sr–Nd–Pb isotope data

Sr and Nd isotopic data are given in Table 3, and Pb isotopic data in Table 4. All isotope data for Emperor Seamount lavas shown in the following figures have been corrected for radioactive decay since eruption; ε_{Sr} and ε_{Nd} values are reported relative to CHUR. Fields for young lavas from the EPR and the Hawaiian Islands at 80 Ma were calculated assuming $^{87}Rb/^{86}Sr$, $^{147}Sm/^{144}Nd$, $^{238}U/^{204}Pb$ and $^{232}Th/^{204}Pb$ ratios of 0·02, 0·24, 5 and 11 for the source of EPR lavas, and 0·06, 0·21, 11 and 35 for the source of Hawaiian lavas (White, 1993; Cohen & O'Nions, 1994; Hémond *et al.*, 1994*b*; Sims *et al.*, 1995; Mahoney *et al.*, 1998).

Meiji Seamount

Initial ε_{Sr} values of the Meiji tholeiitic basalts are lower than those of any tholeiites yet reported from the Hawaiian Islands. The Meiji tholeiites plot at the depleted end of the field for tholeiitic lavas from the Hawaiian Islands in Fig. 5. Sr and Nd isotopic compositions of the single Meiji sample analysed by Keller *et al.* (2000) fall within the range of our samples. Age-corrected Pb isotope compositions lie at the unradiogenic end of the array defined by young lavas from the Hawaiian Islands in Fig. 6, but compared with Hawaiian lavas, have higher $^{208}Pb/^{204}Pb$ for a given $^{206}Pb/^{204}Pb$. The Meiji sample analysed by Keller *et al.* (2000) has similar $^{207}Pb/^{204}Pb$ and $^{208}Pb/^{204}Pb$ ratios to our samples, but significantly higher $^{206}Pb/^{204}Pb$ (Fig. 6). The age correction for the Meiji lavas is relatively large (85 Ma), and some uncertainty in the age correction for these highly altered and strongly leached samples may account for the apparent scatter in Fig. 6. Data for Meiji lavas overlap with the field defined by Hawaiian alkalic lavas in terms of their Pb–Sr–Nd isotopic compositions, but extend to lower $^{206}Pb/^{204}Pb$ (Fig. 7).

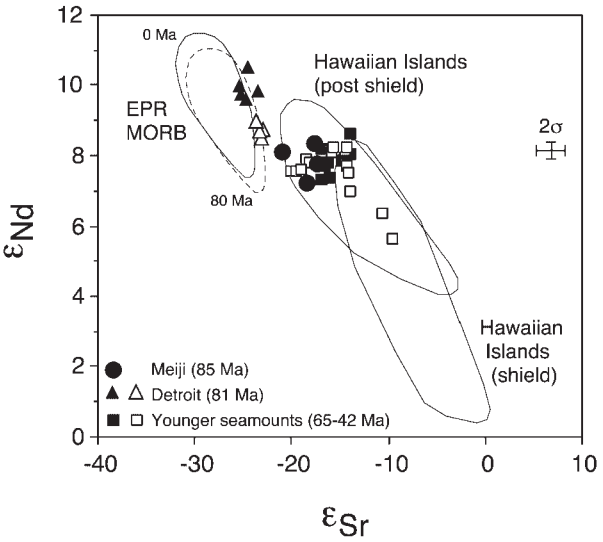

Fig. 5. Initial ε_{Sr} and ε_{Nd} ratios of lavas from the Emperor Seamounts. Fields for tholeiitic and alkalic lavas from the Hawaiian Islands (GEOROC geochemical database: http://georoc.mpch-mainz.gwdg.de) are shown for comparison. Field for MORB from the northern East Pacific Rise (data from Macdougall & Lugmair, 1986; Niu *et al.*, 1999; Regelous *et al.*, 1999; Castillo *et al.*, 2000) calculated at 80 Ma assuming that the mantle source of these lavas has $^{87}Rb/^{86}Sr$ and $^{147}Sm/^{144}Nd$ ratios of 0·02 and 0·24, respectively. Filled symbols for tholeiitic lavas; open symbols for alkalic and transitional lavas.

Detroit Seamount

The Detroit tholeiites have lower initial ε_{Sr} and higher ε_{Nd} than all other Hawaiian–Emperor lavas (Fig. 5). Sr and Nd isotopic compositions of these lavas overlap with those of Pacific N-MORB, but the Detroit tholeiites are displaced to the high ε_{Sr} side of the field for Pacific MORB, and lie on an extension of the Hawaiian Islands array in Fig. 5. Mahoney *et al.* (1998) observed a similar result for leached, old, highly altered basalts, and attributed this to incorporation of non-magmatic Sr into the crystal structure during replacement of plagioclase by secondary feldspar. However, plagioclase phenocrysts in the Detroit tholeiites show no evidence of replacement, and plagioclase-phyric and aphyric samples have similar Sr isotope compositions, indicating that ε_{Sr} ratios of the leached samples are not affected by alteration. Unlike young Hawaiian lavas, the Detroit tholeiites have lower ε_{Sr} and higher ε_{Nd} than the transitional lavas from the same seamount. The low ε_{Sr} and high ε_{Nd} ratios of

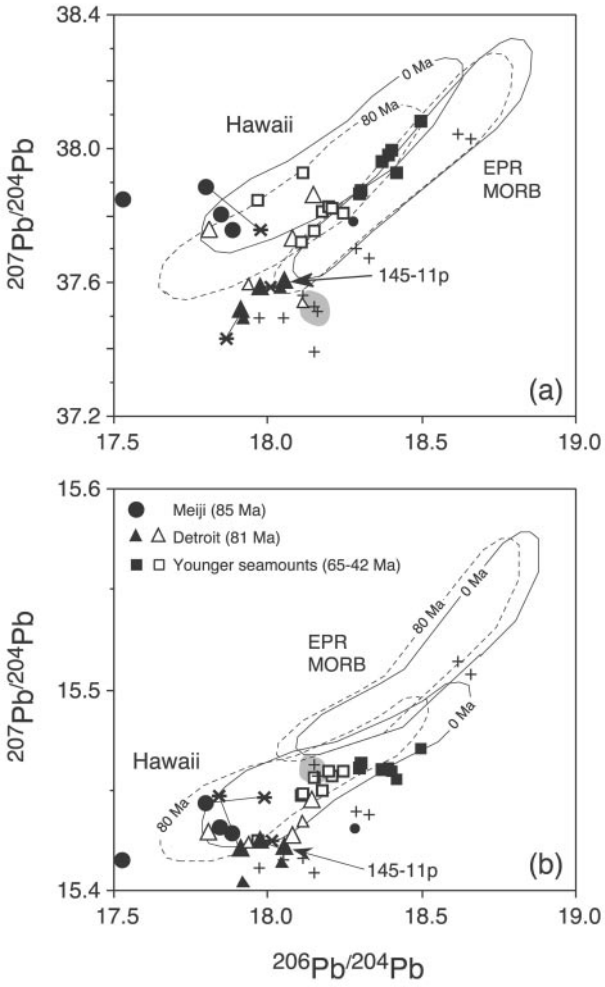

Fig. 6. Initial Pb isotope compositions of leached Emperor Seamount lava samples. Filled symbols for tholeiitic lavas; open symbols for alkalic and transitional lavas. 145-11p is the measured Pb isotope composition of a plagioclase separate from sample 145-11. Stars represent data for unleached rock powders of samples 19-1, 145-10 and 145-11, and connecting lines indicate data for leached powders of the same samples. Fields for triple-spike Pb isotope data for lavas from the Hawaiian Islands and the EPR (Galer *et al.*, 1999; Abouchami *et al.*, 2000; W. Abouchami & S. J. G. Galer, unpublished data, 2002); the dashed fields show compositions at 80 Ma, assuming source $^{238}U/^{204}Pb$ and $^{232}Th/^{204}Pb$ ratios of five and 11 (EPR) and 11 and 35 (Hawaii). +, data for Mesozoic Pacific MORB at 60 Ma (Janney & Castillo, 1997); the shaded field indicates samples of MORB from the Pacific–Farallon spreading centre. Also plotted are conventional Pb isotope data from Keller *et al.* (2000) for Meiji (small circles) and Detroit (small triangles). 2σ errors on the triple-spike measurements (except for 145-11p) are smaller than symbol size.

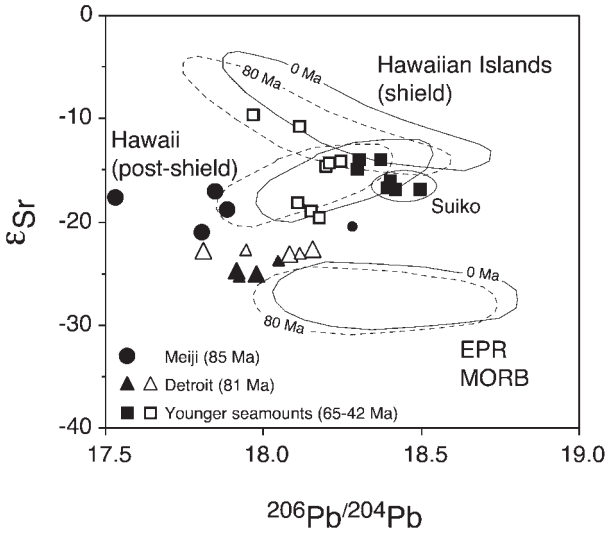

Fig. 7. Variation of ε_{Sr} with initial $^{206}Pb/^{204}Pb$, for lavas from the Emperor Seamounts, the Hawaiian Islands and the East Pacific Rise (data sources as for Fig. 5). Small triangles and small circles are data from Keller *et al.* (2000) for Detroit and Meiji, respectively. Filled symbols for tholeiitic lavas; open symbols for alkalic and transitional lavas. Dashed fields show the compositions of Hawaiian and EPR lavas at 80 Ma.

the Detroit lavas are unusual for intra-plate volcanics, although lavas with similar compositions have been reported from Iceland and the Galapagos Islands (Hémond *et al.*, 1993; White *et al.*, 1993).

The Detroit Seamount lavas have initial $^{206}Pb/^{204}Pb$ ratios within the range of lavas from the Hawaiian Islands (Fig. 6). Compared with young Hawaiian lavas, the Detroit lavas have lower $^{207}Pb/^{204}Pb$ and $^{208}Pb/^{204}Pb$ for a given $^{206}Pb/^{204}Pb$. The transitional lavas from Site 883 have higher $^{208}Pb/^{204}Pb$ than the tholeiitic lavas from Site 884. New high-precision triple-spike isotope measurements (Abouchami *et al.*, 2000; S. J. G. Galer *et al.*, unpublished data, 2002) show that lavas from the Hawaiian Islands and the EPR show little overlap in Pb isotope diagrams (Fig. 6). Compared with EPR MORB, the Detroit lavas have lower $^{207}Pb/^{204}Pb$ for a given $^{206}Pb/^{204}Pb$, but overlap with the unradiogenic end of the MORB field in the $^{206}Pb/^{204}Pb$–$^{208}Pb/^{204}Pb$ diagram (Fig. 6).

Younger seamounts (62–42 Ma)

Tholeiitic basalts from Suiko Seamount have lower initial ε_{Sr} values than tholeiites from the Hawaiian Islands, and tholeiites from younger seamounts (Ojin, Koko and Yuryaku) have ε_{Sr} ratios that lie at the depleted end of the field for Hawaiian lavas (Fig. 5). None of the ESC tholeiites have the high ε_{Sr} and low ε_{Nd} ratios that characterize young shield lavas from Koolau and Lanai. Alkalic lavas from Suiko, Nintoku, Ojin, Koko, Kimmei, Yuryaku and Daikakuji Seamounts have Sr and Nd isotopic compositions within the range found in young Hawaiian post-shield lavas (Fig. 5). Transitional basalts from Daikakuji Seamount at the southern end of the ESC have the highest ε_{Sr} and lowest ε_{Nd} values of all the samples analysed. Tholeiitic lavas from Suiko, Koko and Yuryaku Seamounts all have higher initial $^{87}Sr/^{86}Sr$ than

the associated alkalic lavas; however, the single tholeiite recovered from Ojin Seamount has lower initial $^{87}Sr/^{86}Sr$ ratio than hawaiites from the same seamount.

Our Sr isotope data for these seamounts are similar to those measured by Lanphere *et al.* (1980); however, in our dataset the intra-seamount variation is smaller, and values for dredged lavas are generally shifted to less radiogenic values. This is probably due to the fact that our measurements were carried out on leached sample powders, and therefore more closely reflect the original magmatic values. The single Suiko sample analysed by Keller *et al.* (2000) has age-corrected Sr, Nd and Pb isotope ratios within the range shown by our data.

Initial Pb isotope compositions of tholeiitic and alkalic lavas from Suiko, Nintoku, Ojin, Koko, Kimmei, Yuryaku and Daikakuji Seamounts lie within the field for young lavas from the Hawaiian Islands (Fig. 6). Alkalic lavas generally have less radiogenic Pb isotope compositions than tholeiitic lavas from the same seamount. Compared with the other southern Emperor Seamount lavas, the two transitional lavas from Daikakuji have high $^{208}Pb/^{204}Pb$ for a given $^{206}Pb/^{204}Pb$.

In the $^{206}Pb/^{204}Pb$–ε_{Sr} diagram, tholeiitic lavas from Suiko plot at the high $^{206}Pb/^{204}Pb$ end of the field for Hawaiian Islands tholeiites, with lower $^{87}Sr/^{86}Sr$ (Fig. 7). An alkalic basalt from Suiko Seamount, as well as tholeiitic and alkalic lavas from seamounts younger than 60 Ma (Ojin, Koko, Yuryaku and Daikakuji) lie within the field for Hawaiian lavas.

CHEMICAL AND ISOTOPIC EVOLUTION OF HAWAIIAN MAGMATISM

Figure 8 compares the compositions of lavas from the Emperor Seamounts (85–43 Ma) with those of lavas from the Hawaiian Chain (<43 Ma), to illustrate the temporal chemical and isotopic changes in Hawaiian magmatism. Tholeiites from Meiji Seamount (85 Ma) have low concentrations of incompatible elements, and depleted trace element and Sr isotope ratios, compared with young Hawaiian Islands tholeiites. At 81 Ma, when Detroit Seamount was built, Hawaiian magmatism was even more depleted. Incompatible trace element compositions and Sr and Nd isotope compositions of Detroit tholeiites are unlike those of all other Hawaiian lavas, and are similar to those of Pacific N-MORB. Tholeiitic and alkalic lavas from Emperor Seamounts younger than 65 Ma (Suiko, Nintoku, Ojin, Koko, Kimmei, Yuryaku and Daikakuji) have trace element compositions that lie within the range of young lavas from the Hawaiian Islands. However, between 81 and 42 Ma, there appears to have been a systematic increase in initial ε_{Sr} of both tholeiitic and alkalic lavas (Fig. 8). Between 42 Ma and the present, there has not been any systematic temporal variation in trace element or isotopic composition of Hawaiian magmatism.

The isotope variation within lavas from the Hawaiian Islands has often been explained in terms of mixing of least three end-member components (Staudigel *et al.*, 1984; Stille *et al.*, 1986; Roden *et al.*, 1994; Eiler *et al.*, 1996). However, recent high-precision Pb isotope data indicate that, in detail, many more than three end-members would be required (Abouchami *et al.*, 2000; Eisele *et al.*, in preparation). Our data show that lavas erupted between 56 and 43 Ma had similar Sr–Nd–Pb isotope compositions to lavas from the Hawaiian Islands (although none of the Emperor Seamount lavas analysed in this study has the high ε_{Sr} and low ε_{Nd} ratios that characterize young tholeiites from Lanai and Koolau). The same sources may therefore have contributed to Hawaiian magmatism during this period. Tholeiitic lavas from Suiko Seamount have some of the highest $^{206}Pb/^{204}Pb$ ratios of all Hawaiian lavas (Fig. 7). It has been suggested that the high $^{206}Pb/^{204}Pb$ ('Kea') component is derived from the underlying Pacific lithosphere (Tatsumoto, 1978; Stille *et al.*, 1986). However, Abouchami *et al.* (2000) and Eisele *et al.* (in preparation) have shown that young Kea-type lavas have different Pb isotopic compositions from young Pacific MORB. Our Pb isotope data suggest further that the Kea component is unlikely to be aged Pacific lithosphere, as suggested by Tatsumoto (1978), because Suiko Seamount was built on oceanic lithosphere that was only 40 Myr old (compared with 90–100 Myr old beneath Mauna Kea). Thus, the 'Kea' component is present in both Suiko and Mauna Kea lavas, and appears to be unrelated to the age of the underlying lithosphere. Meiji lavas lie on an extension of the Hawaiian Islands post-shield lava array, but the Detroit lavas are displaced to lower ε_{Sr} and higher ε_{Nd} for a given $^{206}Pb/^{204}Pb$ ratio, compared with young Hawaiian lavas (Fig. 7). This suggests that between 85 and 81 Ma at least one additional source, having low $^{206}Pb/^{204}Pb$ and $^{87}Sr/^{86}Sr$ but high $^{143}Nd/^{144}Nd$ ratios, contributed to Hawaiian tholeiitic magmatism.

A DEPLETED UPPER-MANTLE SOURCE IN CRETACEOUS HAWAIIAN LAVAS?

If the depleted compositions of the oldest Emperor lavas are due to mixing of Hawaiian plume material with the upper-mantle source of MORB, either by entrainment of Pacific upper mantle into the Cretaceous Hawaiian plume, or by plume–spreading ridge interaction (see below), then depleted Pacific-type upper mantle will be one component in the source of these lavas.

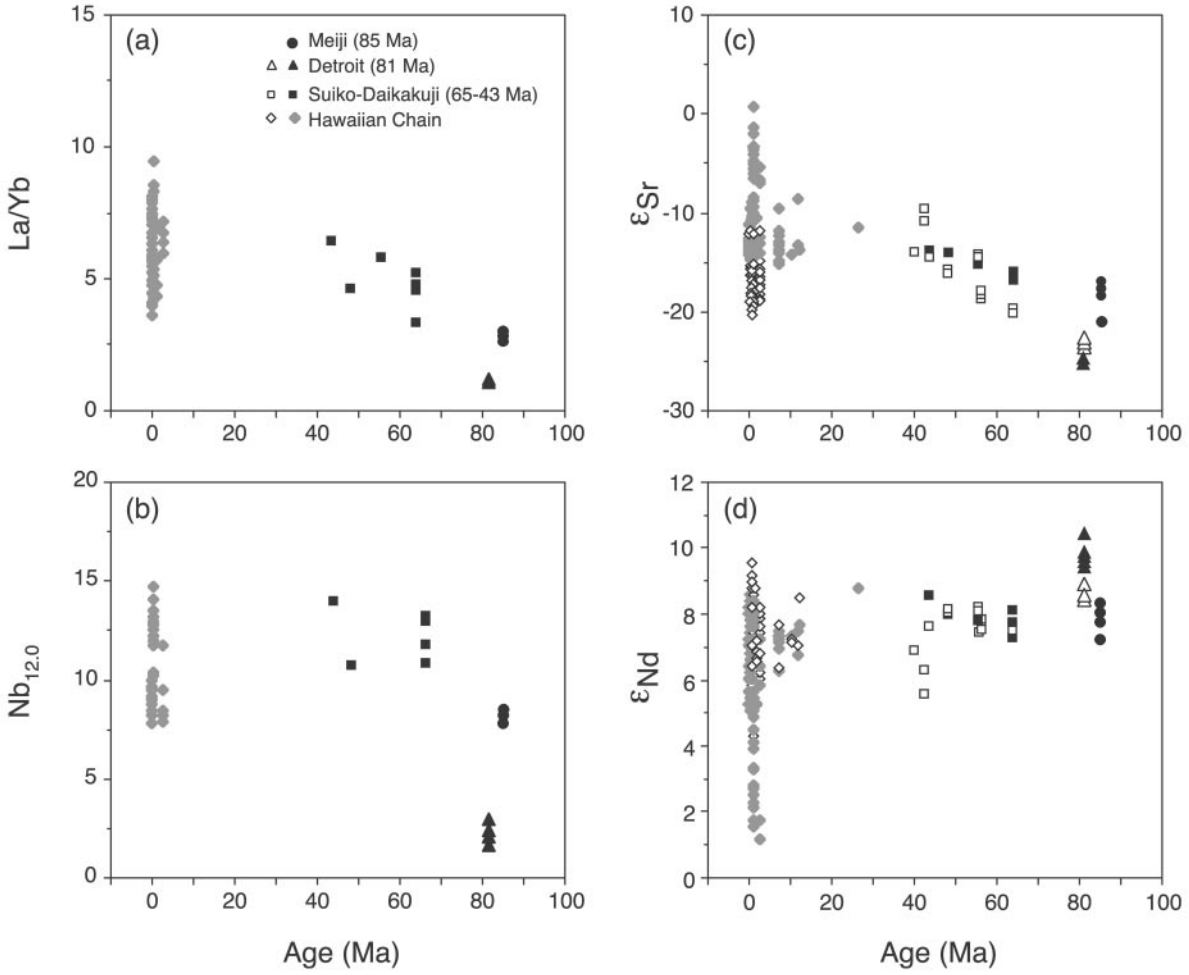

Fig. 8. Variation of (a) La/Yb and (b) $Nb_{12·0}$ of Hawaiian tholeiites with age. $Nb_{12·0}$ is the Nb concentration corrected to a MgO content of 12%, assuming fractionation of olivine with 47·5% MgO (Hofmann & Jochum, 1996). (c) and (d) show variation in ε_{Sr} and ε_{Nd} of Hawaiian–Emperor lavas since 85 Ma [data for Hawaiian Seamounts from Basu & Faggart (1996)]. It should be noted that ε_{Sr} of both alkalic and tholeiitic lavas increased from 81 to 43 Ma. Filled symbols for tholeiitic lavas; open symbols for alkalic and transitional lavas.

The Detroit tholeiites have incompatible element compositions that are broadly similar to those of young Pacific MORB from the northern EPR (Figs 3 and 4). If the Detroit tholeiites are interpreted as melts of such a mixed source, then their Sr isotope compositions (and incompatible trace element ratios) imply that the source is dominated (~90%) by the depleted upper-mantle component, even if a relatively low ε_{Sr} value is assumed for the enriched end-member (Fig. 9a). However, the isotopic compositions of the Meiji and Detroit tholeiites are not entirely consistent with such mixing. Sr and Nd isotope ratios of the Detroit tholeiites overlap with values for Pacific MORB, but the former have higher ε_{Sr} for a given ε_{Nd}, and lie on an extension of the Hawaiian Islands array (Fig. 5). Although sample powders for Sr isotope analysis were strongly acid leached, it is possible that apparent differences in ε_{Sr} values for Detroit tholeiites and Pacific MORB are the result of alteration. However, combined Hf–Nd isotope variations in Detroit and Meiji lavas also appear to be inconsistent with mixing between Hawaiian plume mantle and depleted Pacific upper mantle (Kempton & Barry, 2001), and these elements are much less susceptible to seawater alteration. Compared with East Pacific Rise MORB (excepting the highly depleted lavas from the Garrett Transform; Wendt *et al.*, 1999), the Detroit lavas have lower $^{207}Pb/^{204}Pb$ and slightly higher $^{208}Pb/^{204}Pb$ for a given $^{206}Pb/^{204}Pb$. It should be noted that the measured $^{207}Pb/^{204}Pb$ ratios of the Detroit lavas (15·43–15·46) are lower than most Pacific MORB measured using the triple-spike technique (15·47–15·58), which indicates that uncertainty in the age correction is not responsible for the difference in $^{207}Pb/^{204}Pb$ between Detroit lavas and young Pacific MORB. Two samples of Mesozoic Pacific MORB from

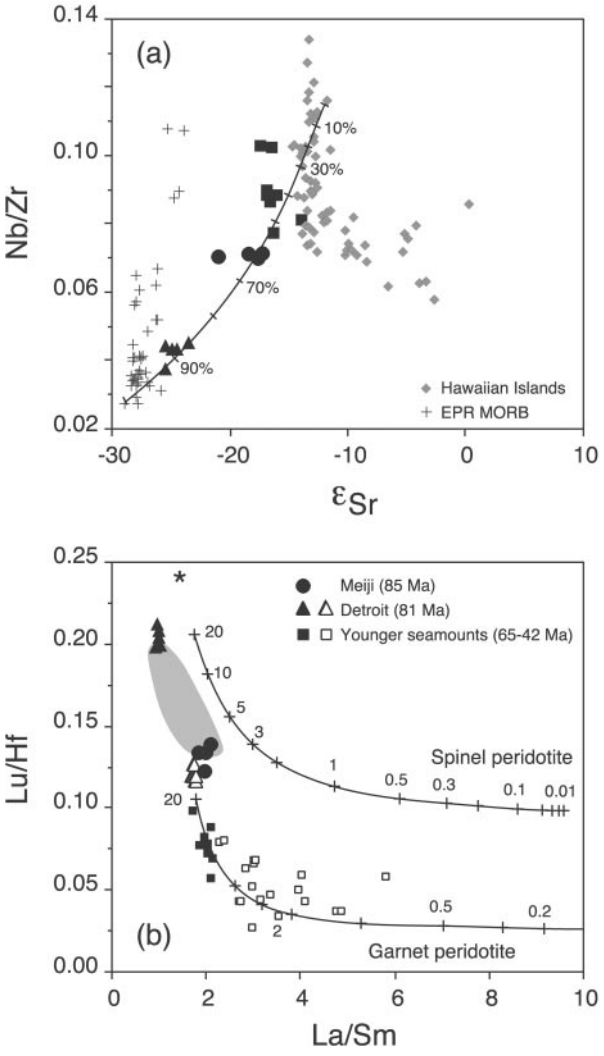

Fig. 9. Variation of (a) Nb/Zr with $^{87}\varepsilon_{Sr}/^{86}\varepsilon_{Sr}$, and (b) Lu/Hf with La/Sm in ESC lavas. The curve in (a) shows effect of mixing between EPR MORB and Hawaiian lava. If the variations in composition of ESC tholeiites are interpreted as the result of mixing between plume and depleted upper mantle, about 85–95% of the latter component is required to account for the highly depleted compositions of the Detroit tholeiites. The curves in (b) show the effect of between 0·01% and 20% equilibrium melting of spinel and garnet peridotite. The source (star) has primitive mantle composition (Sun & McDonough, 1989); partition coefficients are from Salters (1996). Although most of the Emperor lavas are likely to be mixtures of melts of both spinel and garnet peridotite, the low Sm/Yb and high Lu/Hf ratios of the Detroit tholeiites require relatively large degrees of melting within the spinel stability field, of a source with lower La/Sm than primitive mantle. Field in (b) shows range of northern EPR MORB (Niu *et al.*, 1999; Regelous *et al.*, 1999).

DSDP Site 307 (Janney & Castillo, 1997), which, like the oceanic crust underlying the ESC, was emplaced at the Pacific–Farallon spreading axis, also have $^{207}Pb/^{204}Pb$ ratios that are higher than those of the Detroit lavas (Fig. 6). On the other hand, Mesozoic Pacific MORB from DSDP Sites 303 and 304 (Pacific–Izanagi spreading centre) have Pb isotope compositions that overlap with those of the Detroit lavas (Fig. 6).

In summary, the differences in isotopic composition between the depleted Detroit tholeiites and lavas from both active and extinct Pacific spreading centres are not readily explained by mixing between Hawaiian plume mantle and depleted Pacific upper mantle. We suggest that the depleted mantle component that contributes to Detroit and Meiji lavas may be intrinsic to the Hawaiian plume. A depleted plume component has also been identified in intra-plate lavas from the Galapagos (Hoernle *et al.*, 2000) and from Iceland (Thirlwall, 1995; Fitton *et al.*, 1997; Kempton *et al.*, 2000), where it has been argued to represent recycled oceanic lithosphere (Chauvel & Hémond, 2000; Skovgaard *et al.*, 2001). The non-primitive (high) Nb/Th ratios of the Detroit tholeiites (Fig. 4), together with their unradiogenic Sr and Pb isotopic compositions and high ε_{Nd} values, are at least consistent with ancient, subducted lower oceanic lithosphere being the depleted component in the Hawaiian plume (Hofmann & White, 1982).

ORIGIN OF TEMPORAL CHEMICAL AND ISOTOPIC VARIATIONS

Explanations for the temporal changes in Hawaiian magmatism must be able to account for (1) the highly depleted trace element and isotopic compositions of both tholeiitic and alkalic lavas from the oldest Emperor Seamounts, (2) the fact that such depleted lavas occur on the ESC but not the Hawaiian Chain, (3) the apparent systematic increase in initial ε_{Sr} values of both tholeiitic and alkalic lavas from 81 to 43 Ma, and (4) the observation that the incompatible element depleted Detroit tholeiites have different isotope compositions from those of most Pacific MORB.

Changes in mantle plume composition

A possible explanation for the unusual compositions of the oldest Emperor Seamount lavas is that the composition of the mantle ascending in the Hawaiian plume has changed over time. The total volume of magma erupted between 85 and 42 Ma was $\sim 5 \times 10^5$ km^3 (Bargar & Jackson, 1974). If Hawaiian lavas represent $\sim 7\%$ melting (Watson & McKenzie, 1991), then the volume of mantle that has been processed through the plume during this period is of the order of 3×10^6 km^3. Plume mantle that was heterogeneous on length-scales of 100–1000 km could therefore account for variations in the chemistry of erupted lavas over time scales of 10–100 Ma (Janney & Castillo, 1999). On the other hand, tholeiitic lavas as depleted as those from Detroit Seamount are rare on

other intra-plate seamount chains, and have not been found on the Hawaiian Chain. Nevertheless, it is difficult to rule out a change in source composition as an explanation for the temporal variations in Hawaiian magmatism.

Class *et al.* (1993) have argued that changes in the isotope compositions of lavas along the Ninetyeast Ridge (Indian Ocean) reflect radioactive decay within the mantle source of the lavas. However, this process cannot account for the observed variations of $^{87}Sr/^{86}Sr$ along the Hawaiian–Emperor Chain, because there is not a simple progression to higher ε_{Sr} with decreasing age (Fig. 8). Furthermore, an unrealistically high Rb/Sr ratio ($\sim$0·213) would be required for the ε_{Sr} value of the mantle source to evolve from -26 to -15 between 81 and 43 Ma (Fig. 8). In addition, radioactive decay in the source of the lavas cannot account for the higher (more radiogenic) ε_{Nd} ratios of the Detroit lavas compared with those of younger Emperor lavas (Fig. 8), nor the relatively depleted incompatible trace element compositions of the Meiji and Detroit lavas.

Plume–spreading ridge interaction

The Hawaiian Islands and the Hawaiian Seamounts are situated on oceanic lithosphere that was 80–100 Myr old at the time of intra-plate magmatism (Caplan-Auerbach *et al.*, 2000) (Fig. 10). The difference in age between the seamount and the underlying crust decreases northwards along the Emperor Seamount Chain, from $\sim$80 Ma at Daikakuji Seamount, to $\sim$40 Ma at Suiko Seamount (Fig. 10). The northern Emperor Seamounts were constructed on young oceanic crust close to a former spreading centre between the Pacific and Kula, or Farallon Plates (Rea & Dixon, 1983; Lonsdale, 1988*a*; Mammerickx & Sharman, 1988). The age of the ocean floor beneath the northernmost Emperor Seamounts is not well constrained, because it was formed during the Cretaceous Quiet Period and therefore lacks magnetic lineations. However, the absence of a flexural moat close to the Obruchev Rise, the relatively low gravity signal around Meiji (Sandwell & Smith, 1997) and the low heights of Detroit and Meiji guyots (Caplan-Auerbach *et al.*, 2000), suggest that the oldest Emperor Seamounts were formed on thin lithosphere that was <20 Myr old at that time.

Lanphere *et al.* (1980) have proposed that variations in the distance to a former spreading centre could explain the isotopic changes along the Emperor Seamount Chain, and Keller *et al.* (2000) argued that such changes resulted from plume–ridge interaction. Plumes are known to influence the composition of lavas erupted at nearby spreading ridges (Schilling *et al.*, 1985; Hanan *et al.*, 1986). Conversely, hotspots located close to active spreading ridges often erupt lavas with relatively depleted compositions (Hémond *et al.*, 1993; White *et al.*, 1993; Haase *et al.*, 1996; Hékinian *et al.*, 1999). However, the physical process of plume–ridge interaction is not well understood. Two possible mechanisms, which have been used to explain the depleted compositions of lavas from Easter Island and its vicinity, are formation within a sublithospheric channel between the plume and the nearby ridge axis (Kingsley & Schilling, 1998), and flow of mantle material from the spreading ridge towards the plume (Haase *et al.*, 1996).

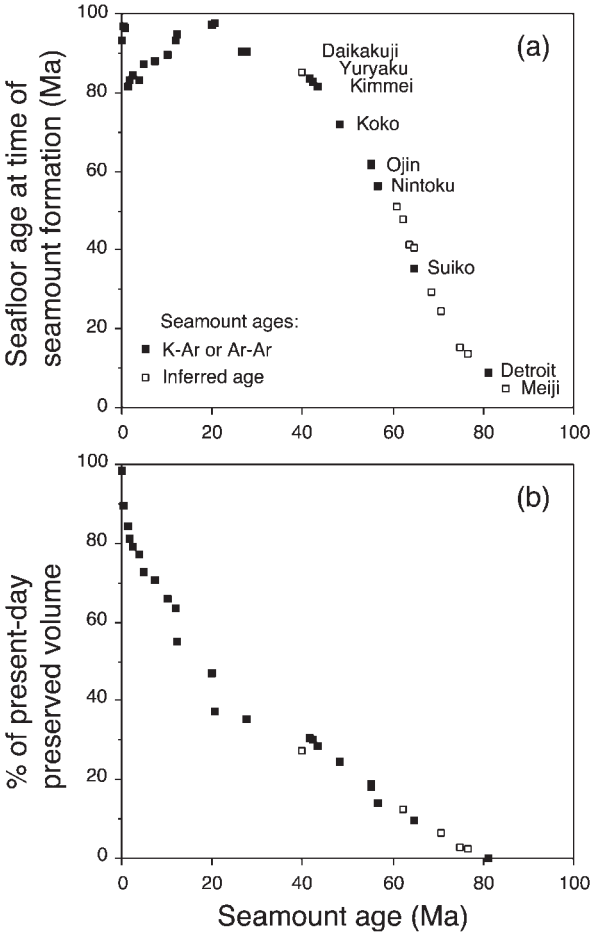

Fig. 10. (a) Variation in age of Pacific lithosphere (at the time of formation of each seamount) underlying the Hawaiian–Emperor Seamount Chain. Data from Caplan-Auerbach *et al.* (2000). (b) Cumulative increase with time in volume of Hawaiian shield volcanoes from Detroit Seamount [volume data from Bargar & Jackson (1974); inferred seamount ages from Caplan-Auerbach *et al.* (2000)].

The ages of individual seamounts of the Emperor Chain increase progressively from south to north, which indicates that the oldest seamounts were not formed in a plume channel. Bi-directional flow and mixing of material between the plume and the ridge axis is an unlikely explanation for the compositions of the Meiji and Detroit tholeiites, because the highly depleted trace element and isotopic compositions of the latter (Fig. 9)

would require the flow of material from ridge to plume to dominate the flow from plume to ridge.

Keller *et al.* (2000) suggested that beneath young, thin oceanic lithosphere, the melting column extends to shallower depths, and the ratio of depleted asthenosphere to enriched plume mantle that is melted may be larger. Alternatively, increased entrainment of depleted upper-mantle material into a plume may occur when the plume is close to a spreading centre (Keller *et al.*, 2000). However, neither of these mechanisms can explain satisfactorily the isotopic compositions of the oldest Emperor lavas. As discussed previously, assuming that the North Pacific mantle at 80 Ma was similar in composition to that sampled along the length of the EPR (and taking into account the effects of radioactive decay), the combined Sr–Nd and Nd–Hf isotopic compositions of Detroit and Meiji lavas appear to be inconsistent with mixing between Pacific depleted upper mantle and Hawaiian plume mantle. Detroit lavas also have different Pb isotope compositions from those of both young lavas from the EPR and Mesozoic MORB from the Pacific–Farallon spreading centre. Moreover, it is unlikely that plume–ridge interaction of any form could explain the systematic increase in ε_{Sr} that occurred from 81 to 43 Ma (Fig. 8; Lanphere *et al.*, 1980), because the age difference between the youngest Emperor Seamounts and the underlying oceanic lithosphere is about 80 Ma (Fig. 10). This age difference would correspond to a plume–ridge distance of over 3000 km at the time the southern Emperor Seamounts were constructed. The Suiko tholeiites have lower ε_{Sr} than young Hawaiian tholeiites (Fig. 5), yet Suiko Seamount was built on 40 Myr old lithosphere. Plume–ridge interaction has not previously been proposed for distances of more than $\sim$1700 km (Schilling *et al.*, 1985; Schilling, 1991), and it is therefore unlikely that a ridge could influence the chemistry of hotspot lavas over such a distance.

LITHOSPHERE THICKNESS AS A CONTROL ON MANTLE UPWELLING AND MELTING

Intra-plate lavas erupted onto younger, thinner lithosphere are produced by larger mean degrees of melting, at shallower average depth, than melts produced beneath thicker lithosphere. This is because the overlying lithosphere acts as a 'lid' that restricts the upper boundary of the melting column during decompression melting (Ellam, 1992; Haase, 1996). Both the degree and the depth of melting influence the chemistry of intra-plate magmas. For the same MgO, the Detroit and Meiji tholeiites have lower Fe contents than other Emperor Seamount tholeiites (Fig. 2), consistent with relatively high degrees of melting at low pressure beneath a thin lithosphere (Jaques & Green, 1980).

Variations in the depth of melting may also influence the trace element chemistry of intra-plate lavas, according to how much of the melting occurs within the stability field of garnet (Ellam, 1992; Haase, 1996). The Detroit tholeiites have low La/Yb and high Lu/Hf ratios compared with other Hawaiian–Emperor tholeiites and most EPR MORB (Figs 4 and 9). The trace element compositions of the Detroit tholeiites indicate that they are the product of relatively high degrees of mantle melting, and that much of the melt was generated at low pressure, within the stability field of spinel (Fig. 9). Larger mean degrees of melting beneath thin oceanic lithosphere may to some extent explain the low incompatible element concentrations of the Detroit and Meiji lavas. On the other hand, there is no indication from the volumes of Hawaiian–Emperor volcanoes that the average degree of mantle melting was greater before 60 Ma (Fig. 10).

Clearly, variable melting of a homogeneous source cannot explain the variations in highly incompatible trace element and isotope ratios in Emperor Seamount lavas. We suggest instead that the temporal variations in Emperor lava composition may be the result of variable degrees of disequilibium melting of heterogeneous plume mantle as a result of variations in the thickness of the overlying lithosphere (Fig. 11). Several workers have suggested that the mantle consists of low melting point, incompatible element enriched heterogeneities embedded in a more depleted, refractory matrix (Sun & Hanson, 1975; Sleep, 1984; Allègre & Turcotte, 1986; Phipps Morgan & Morgan, 1999; Niu *et al.*, 1999, 2001; Hoernle *et al.*, 2000). Phipps Morgan (1999) has argued that disequilibrium melting of a heterogeneous mantle may account for some of the isotopic heterogeneity observed in the lavas from individual oceanic islands, and the fact that these often define tube-like arrays in three-dimensional isotope space. With progressive melting of such a heterogeneous mantle, as a result of an increasingly thin lithosphere, the melts produced would have increasingly lower incompatible trace element contents, lower ratios of more- to less-incompatible elements, lower $^{87}Sr/^{86}Sr$, and higher $^{143}Nd/^{144}Nd$ (Phipps Morgan, 1999). This hypothesis predicts variations in basalt chemistry with lithospheric thickness that are qualitatively similar to those observed along the ESC. In detail, the melt extraction trajectories created during this process are sensitive to the compositions and ease of melting of the various source components, although it is interesting that the Detroit lavas plot close to the end of the melting trajectory estimated for Hawaiian plume mantle by Phipps Morgan (1999). Phipps Morgan & Morgan (1999) suggested that MORB are the result of melting residual mantle created by melting beneath oceanic islands but, as discussed above, the Detroit tholeiites have different

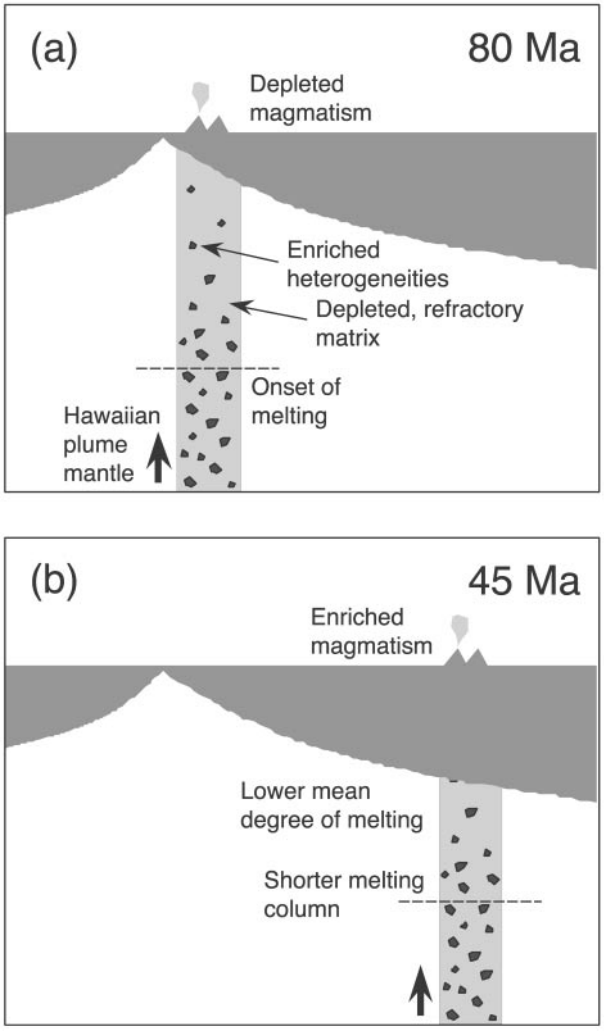

Fig. 11. Schematic diagrams illustrating how the thickness of the lithosphere may have influenced the incompatible trace element and isotope compositions of Hawaiian–Emperor lavas. (a) Depleted compositions of Hawaiian lavas at ~80 Ma are the result of relatively high degrees of melting of a heterogeneous mantle. A greater proportion of the refractory, incompatible element depleted material within the ascending plume mantle is melted, when the plume is situated beneath younger, thinner lithosphere. (b) In contrast, beneath older, thicker oceanic lithosphere, the mean degree of melting is lower, and incompatible element enriched, easily melted mantle components contribute more to the melting.

compositions from those of MORB. We suggest that the depleted compositions of the Detroit lavas are the result of melting a relatively refractory component contained within the ascending plume mantle (Fig. 11). This depleted component does not contribute to younger Hawaiian lavas, which were formed by lesser degrees of melting beneath thicker lithosphere. This could explain why the Pb isotopic compositions of the Detroit lavas are unlike those of Pacific MORB. Interestingly, a refractory plume component, which is chemically and isotopically depleted yet distinct from the upper-mantle source of MORB, has been identified in lavas from the Galapagos (Hoernle *et al.*, 2000) and Iceland (Skovgaard *et al.*, 2001), both of which are located on young, thin lithosphere.

Geophysical measurements have shown that the thickness of the oceanic lithosphere increases as a function of age until the lithosphere is about 70 Myr old, after which time the thickness remains approximately constant (Parsons & Sclater, 1977). This could explain why systematic chemical and isotopic variations are observed along the Emperor Seamount Chain (situated on oceanic lithosphere that was <20–70 Myr old at the time of seamount magmatism), but not along the Hawaiian Seamount Chain (where the crust was 70–100 Myr old at the time of seamount magmatism). Variable melting of a heterogeneous mantle can also explain the increase in $^{87}Sr/^{86}Sr$ from 81 to 43 Ma, when the Hawaiian plume was situated up to 3000 km from the nearest spreading axis.

EVIDENCE FROM OTHER SEAMOUNT CHAINS

If lithospheric thickness is an important control on the trace element and isotope composition of intra-plate lavas, then geochemical variations should also occur along other seamount chains that were built upon lithosphere of variable age. Unfortunately, there have not been many detailed studies of the long-term (~100 Myr) geochemical evolution of other seamount chains, and in most cases the variation in age of the underlying lithosphere is even more poorly known.

Volcanic rocks from the Ninetyeast Ridge (~90 Ma to 38 Ma) and Kerguelen Archipelago (~45 Ma to present) in the Indian Ocean record changes in the chemistry of magmatism above the Kerguelen plume. Much of the Ninetyeast Ridge was formed close to the Southeast Indian Ridge, but the ridge axis passed over the hotspot at ~40 Ma, and since that time the hotspot has become progressively distant from the ridge (Royer & Sandwell, 1989). Lavas from the Ninetyeast Ridge have relatively depleted trace element and isotopic compositions and low La/Yb ratios (Frey & Weis, 1995), which may reflect their formation beneath relatively thin lithosphere close to the ridge axis. Younger lavas from the Kerguelen Archipelago, which were erupted onto older, thicker lithosphere, are generally more alkalic and have more enriched trace element and isotope compositions (Gautier *et al.*, 1990; Frey *et al.*, 2000).

The Easter Seamount Chain in the eastern Pacific is ~3000 km long, and the age of magmatism varies from 0 Ma at Easter Island and Salas y Gomes, to ~30 Ma at the eastern end of the chain (Cheng *et al.*, 1999). The age of the underlying crust is not well known, but increases

from 1–4 Ma at Easter Island to 8–10 Ma at Salas y Gomes. Sr, Nd and Pb isotope compositions of the lavas from seamounts at the eastern end of the chain, which were formed on older, thicker lithosphere, tend to be more enriched (Cheng *et al.*, 1999). The age of the underlying lithosphere, and even the exact location of the plume, is not well known.

The Louisville Seamount Chain, in the SW Pacific, ranges in age from 66 Ma at the western end, to 0 Ma at the eastern end. Since 33 Ma, the Louisville plume has been situated on oceanic crust that was 45–52 Myr old at the time of magmatism, whereas estimates of the age of the crust underlying the older (33–66 Ma) seamounts at their time of formation range from 50 to 80 Ma (Lonsdale, 1988*b*; Watts *et al.*, 1988; Lyons *et al.*, 2000). The age-corrected isotopic compositions of lavas from the Louisville Seamounts show little variation (Cheng *et al.*, 1987).

The isotope compositions of lavas erupted along the Pukapuka Ridge in the South Pacific vary with the age of the underlying sea floor, which was between 0 and 25 Myr old, at the time of intra-plate volcanism (Janney *et al.*, 2000). Lavas erupted onto younger sea floor were formed by larger degrees of melting, at lower pressures, and have more depleted compositions than lavas erupted onto older lithosphere. The Pukapuka Ridge was not formed by hotspot activity, but by lithospheric extension (Sandwell *et al.*, 1995), and thus plume–ridge interaction cannot be responsible for the isotopic variations. Instead, these might be the result of variations in distance from the enriched South Pacific Superswell (Janney *et al.*, 2000). Alternatively, they could be the result of differences in the degree of melting of heterogeneous mantle beneath lithosphere of variable thickness.

Intra-plate lavas associated with the Canary hotspot in the NE Atlantic were erupted upon sea floor that was between 90 and 175 Myr old, and show little variation in isotopic composition (Geldmacher *et al.*, 2001). In contrast, systematic temporal isotopic variations occur along the nearby Madeira seamount chain, which was built upon oceanic crust that was ~60 to 130 Myr old, but these isotopic variations appear to be related to contamination by continental lithosphere (Geldmacher & Hoernle, 2000).

In summary, the geochemical variations along other seamount chains are consistent with lithospheric thickness being an important control on the extent of melting of plume mantle, and hence the compositions of the lavas produced. However, detailed geochemical and geochronological studies of other seamount chains, together with more precise constraints on the age of the underlying sea floor, are required, before the influence of lithosphere thickness on the compositions of intra-plate lavas can be fully quantified. Our hypothesis predicts that intra-plate lava chemistry will vary with the thickness of the lithosphere (rather than with plume–ridge distance, as required by plume–ridge interaction). This effect can occur only along those seamount chains where the age difference between the seamounts and the underlying oceanic lithosphere is less than ~70 Myr. This implies that systematic geochemical and isotopic variations may be found along seamount chains that were constructed several thousand kilometres from the nearest spreading axis.

CONCLUSIONS

(1) New major and trace element, and Sr, Nd and Pb isotopic analyses of 44 samples of volcanic rock from nine seamounts along the Hawaiian–Emperor Seamount Chain, provide a 43 Myr record (from ~85 to 42 Ma) of the geochemistry of Hawaiian magmatism, and show that there were large temporal variations in trace element chemistry and isotopic composition of Hawaiian magmatism over this period.

(2) Lavas from the oldest seamounts sampled (Meiji and Detroit) have depleted incompatible trace element and Sr–Nd isotopic compositions, compared with those of young lavas from the Hawaiian Islands. Tholeiitic basalts from Detroit Seamount have incompatible trace element ratios, and Sr–Nd isotope compositions similar to those of modern Pacific mid-ocean ridge basalts, but higher $^{87}Sr/^{86}Sr$ for a given $^{143}Nd/^{144}Nd$. Trace element compositions of Emperor Seamount lavas younger than 62 Ma are similar to those of young Hawaiian lavas, but $^{87}Sr/^{86}Sr$ ratios lie at the depleted end of the Hawaiian Islands array. From 81 to 42 Ma, there was a systematic increase in $^{87}Sr/^{86}Sr$ of both tholeiitic and alkalic lavas erupted above the Hawaiian mantle plume.

(3) Age-corrected Pb isotope compositions of most Emperor lavas lie within the field of young lavas from the Hawaiian Islands. The incompatible element depleted Detroit tholeiites have lower $^{207}Pb/^{204}Pb$ for a given $^{206}Pb/^{204}Pb$, compared with MORB erupted along the East Pacific Rise and at the extinct Pacific–Farallon spreading centre.

(4) The trace element and isotope compositions of these lavas vary with the age of the underlying oceanic Pacific lithosphere at the time of seamount magmatism. The oldest Emperor Seamount lavas, which were erupted onto relatively young lithosphere close to a former spreading centre, have relatively depleted incompatible trace element and isotope compositions. In contrast, younger Hawaiian–Emperor lavas were erupted onto older lithosphere, and have more enriched compositions.

(5) The isotope compositions of the oldest Emperor lavas, together with the fact that the youngest Emperor Seamounts were formed >3000 km from the closest spreading axis, suggest that plume–ridge interaction was

not responsible for the observed chemical and isotopic variations.

(6) Major and trace element compositions of Meiji and Detroit Seamount tholeiites indicate that they were formed by relatively large degrees of mantle melting, at lower pressures, compared with younger ESC tholeiitic lavas.

(7) We suggest that variable degrees of melting of a heterogeneous mantle may explain the temporal compositional changes in Hawaiian magmatism. When the Hawaiian plume was situated beneath young, thin lithosphere, melting was more extensive and extended to shallower depths. The melts produced had relatively depleted trace element and isotope compositions, because incompatible element depleted, more refractory source materials contributed more to the melting. In contrast, lavas from the younger seamounts, which were built on older, thicker crust, are more enriched because they were produced by smaller degrees of melting, and so the compositions of the melts were dominated by the contribution from incompatible-element-rich, easily melted mantle materials.

ACKNOWLEDGEMENTS

This research used samples provided by the Ocean Drilling Program (ODP), which is sponsored by the US National Science Foundation and participating countries under management of Joint Oceanographic Institutions Inc. Warren Smith kindly provided samples from the Geological Collections of the Scripps Institution of Oceanography. We thank F. Frey, M. Garcia, an anonymous reviewer, and the editor M. Thirlwall for constructive comments, which improved the manuscript. M.R. thanks Y. Niu, J. Lassiter and I. Vlastélic for discussions and ideas, A. Greig for the trace element analyses, and S. Bederke-Raczek and H. Feldmann for technical assistance. This research was supported by the DFG and MPI.

REFERENCES

Abouchami, W., Galer, S. J. G. & Hofmann, A. W. (2000). High precision lead isotope systematics of lavas from the Hawaiian Scientific Drilling Project. *Chemical Geology* **169**, 187–209.

Allègre, C. J. & Turcotte, D. L. (1986). Implications of a two-component marble-cake mantle. *Nature* **323**, 123–127.

Bargar, R. E. & Jackson, E. D. (1974). Calculated volumes of individual shield volcanoes along the Hawaiian–Emperor Chain. *US Geological Survey Journal of Research* **2**, 545–550.

Basu, A. R. & Faggart, B. E. (1996). Temporal isotopic variation in the Hawaiian mantle plume: the Lanai Anomaly, the Molokai Fracture Zone, and a seawater-altered lithospheric component in Hawaiian volcanism. In: Basu, A. & Hart, S. R. (eds) *Earth Processes: Reading the Isotopic Code. Geophysical Monograph, American Geophysical Union* **95**, 149–159.

Bence, A. E., Taylor, S. R. & Fisk, M. (1980). Major and trace element geochemistry of basalts from Ojin, Nintoku and Suiko Seamounts of the Emperor Seamount Chain: DSDP–IPOD Leg 55. In: Jackson, E.D., Kosumi, I. *et al.* (eds), *Initial Reports of the Deep Sea Drilling Project, 55*. Washington, DC: US Government Printing Office, pp. 599–605.

Caplan-Auerbach, J., Duennebier, F. & Ito, G. (2000). Origin of intraplate volcanoes from guyot heights and oceanic palaeodepth. *Journal of Geophysical Research* **105**, 2679–2697.

Castillo, P. R., Klein, E., Bender, J., Langmuir, C., Shirey, S., Batiza, R. & White, W. (2000). Petrology and Sr, Nd, Pb isotope geochemistry of mid-ocean ridge basalt glasses from the 11°45′N to 15°00′N segment of the East Pacific Rise. *Geochemistry, Geophysics, Geosystems* **1**, paper 1999GC000024.

Chauvel, C. & Hémond, C. (2000). Melting of a complete section of recycled oceanic crust: trace element and Pb isotopic evidence from Iceland. *Geochemistry, Geophysics, Geosystems* **1**, paper 1999GC000002.

Chauvel, C., McDonough, W., Guille, G., Maury, R. & Duncan, R. (1997). Contrasting old and young volcanism in Rurutu Island, Austral Chain. *Chemical Geology* **139**, 125–143.

Cheng, Q. C., Park, K.-H., Macdougall, J. D., Zindler, A., Lugmair, G. W., Hawkins, J. W., Lonsdale, P. & Staudigel, H. (1987). Isotopic evidence for a hot spot origin of the Louisville Seamount Chain. In: Keating, B. H., Fryer, P., Batiza, R. & Boehlert, G. W. (eds) *Seamounts, Islands and Atolls. Geophysical Monograph, American Geophysical Union* **43**, 283–296.

Cheng, Q. C., Macdougall, J. D. & Zhu, P. (1999). Isotopic constraints on the Easter Seamount Chain source. *Contributions to Mineralogy and Petrology* **135**, 225–233.

Clague, D. A. & Dalrymple, G. B. (1973). Age of Koko Seamount, Emperor Seamount Chain. *Earth and Planetary Science Letters* **17**, 411–415.

Clague, D. A. & Dalrymple, G. B. (1987). Geologic evolution of the Hawaiian–Emperor volcanic chain. In: Decker, R. W., Wright, T. L. & Stauffer, P. (eds) *Volcanism in Hawaii. US Geological Survey Professional Paper* **1350**, 5–54.

Clague, D. A. & Dalrymple, G. B. (1989). Tectonics, geochronology and origin of the Hawaiian–Emperor Volcanic Chain. In: Winterer, E. L., Hussong, D. M. & Decker, R. W. (eds) *The Geology of North America, Volume N: The Eastern Pacific Ocean and Hawaii*. Boulder, CO: Geological Society of America, pp. 188–217.

Clague, D. A. & Frey, F. A. (1980). Trace element geochemistry of tholeiitic basalts from Site 433C, Suiko Seamount. In: Jackson, E. D. & Kosumi, I. *et al.* (eds). *Initial Reports of the Deep Sea Drilling Project, 55*. Washington, DC: US Government Printing Office, pp. 559–569.

Clague, D. A., Dalrymple, G. B. & Moberly, R. (1975). Petrography and K–Ar ages of dredged volcanic rocks from the western Hawaiian Ridge and the southern Emperor Seamount Chain. *Geological Society of America Bulletin* **86**, 991–998.

Class, C., Goldstein, S. L., Galer, S. J. G. & Weis, D. (1993). Young formation age of a mantle plume source. *Nature* **362**, 715–721.

Cohen, A. & O'Nions, R. K. (1994). Melting rates beneath Hawaii: evidence from uranium series isotopes in recent lavas. *Earth and Planetary Science Letters* **120**, 169–175.

Cohen, R. S. & O'Nions, R. K. (1982). The lead, neodymium and strontium isotopic structure of ocean ridge basalts. *Journal of Petrology* **23**, 299–324.

Dalrymple, G. B. & Clague, D. A. (1976). Age of the Hawaiian–Emperor Bend. *Earth and Planetary Science Letters* **31**, 313–329.

Dalrymple, G. B. & Garcia, M. O. (1980). Age and chemistry of volcanic rocks dredged from Jingu Seamount, Emperor Seamount Chain. In: Jackson, E. D., Kosumi, I. *et al.* (eds) *Initial Reports of the*

Deep Sea Drilling Project 55. Washington, DC: US Government Printing Office, pp. 685–691.

Dalrymple, G. B., Lanphere, M. A. & Jackson, E. D. (1974). Contributions to the petrography and geochronology of volcanic rocks from the Leeward Hawaiian Islands. *Geological Society of America Bulletin* **85**, 727–738.

Dalrymple, G. B., Lanphere, M. A. & Clague, D. A. (1980*a*). Conventional and $^{40}Ar/^{39}Ar$ K–Ar ages of volcanic rocks from Ojin (Site 430), Nintoku (Site 432), and Suiko (Site 433) Seamounts and the chronology of volcanic propagation along the Hawaiian–Emperor Chain. In: Jackson, E. D., Kosumi, I. *et al.* (eds), *Initial Reports of the Deep Sea Drilling Project*, *55*. Washington, DC: US Government Printing Office, pp. 659–676.

Dalrymple, G. B., Lanphere, M. A. & Natland, J. H. (1980*b*). K–Ar minimum age for Meiji Guyot, Emperor Seamount Chain. In: Jackson, E. D., Kosumi, I. *et al.* (eds), *Initial Reports of the Deep Sea Drilling Project*, *55*. Washington, DC: US Government Printing Office, pp. 677–683.

Dalrymple, G. B., Clague, D. A. Garcia, M. O. & Bright, S. W. (1981). Petrology and K–Ar ages of dredged samples from Laysan Island and Northampton Bank volcanoes, Hawaiian Ridge, and evolution of the Hawaiian–Emperor chain. *Geological Society of America Bulletin* **92**, 884–933.

Dupuy, C., Vidal, P., Maury, R. C. & Guille, G. (1993). Basalts from Mururoa, Fangataufa and Gambier Islands (French Polynesia): geochemical dependence on the age of the lithosphere. *Earth and Planetary Science Letters* **117**, 89–100.

Eiler, J. M., Farley, K. A., Valley, J. W., Hofmann, A. W. & Stolper, E. M. (1996). Oxygen isotope constraints on the sources of Hawaiian volcanism. *Earth and Planetary Science Letters* **144**, 453–468.

Ellam, R. M. (1992). Lithospheric thickness as a control on basalt geochemistry. *Geology* **20**, 153–156.

Fisk, M. R., Duncan, R. A., Baxter, A. N., Greenough, J. D., Hargraves, R. B., Tatsumi, Y. & Shipboard Scientific Party (1989). Reunion hotspot magma chemistry over the past 65 M. y.: results from Leg 115 of the ODP. *Geology* **17**, 934–937.

Fitton, J. G., Saunders, A. D., Norry, M. J., Hardarson, B. S. & Taylor, R. N. (1997). Thermal and chemical structure of the Iceland Plume. *Earth and Planetary Science Letters* **153**, 197–208.

Frey, F. A. & Weis, D. (1995). Temporal evolution of the Kerguelen plume: geochemical evidence from ~38 to 82 Ma lavas forming the Ninetyeast Ridge. *Contributions to Mineralogy and Petrology* **121**, 12–28.

Frey, F. A., Garcia, M. O. & Roden, M. F. (1994). Geochemical characteristics of Koolau Volcano: implications of intershield geochemical differences among Hawaiian volcanoes. *Geochimica et Cosmochimica Acta* **58**, 1441–1462.

Frey, F. A., Weis, D., Yang, H.-J., Nicolaysen, K., Leyrit, H. & Giret, A. (2000). Temporal geochemical trends in Kerguelen Archipelago basalts: evidence for decreasing magma supply from the Kerguelen Plume. *Chemical Geology* **164**, 61–80.

Galer, S. J. G. (1999). Optimal double and triple spiking for high precision lead isotopic measurement. *Chemical Geology* **157**, 255–274.

Galer, S. J. G., Abouchami, W. & Macdougall, J. D. (1999). East Pacific Rise MORB through the Pb isotope looking-glass. *EOS Transactions, American Geophysical Union* **80**, F1086.

Garcia, M. O., Grooms, D. G. & Naughton, J. J. (1987). Petrology and geochronology of volcanic rocks from seamounts along and near the Hawaiian Ridge: implications for the propagation of the ridge. *Lithos* **20**, 323–336.

Garcia, M. O., Park, K.-H. & Davies, G. T. (1993). Petrology and isotope geochemistry of lavas from the Line Islands Chain, Central Pacific Basin. In: Pringle, M.S., Sager, W.W., Sliter, W.V. & Stein, S. (eds). *The Mesozoic Pacific: Geology, Tectonics, and Volcanism. Geophysical Monograph, American Geophysical Union* **77**, 217–231.

Gautier, I., Weis, D., Mennessier, J.-P., Vidal, P., Giret, A. & Loubet, M. (1990). Petrology and geochemistry of the Kerguelen Archipelago basalts (South Indian Ocean): evolution of the mantle sources from ridge to intraplate position. *Earth and Planetary Science Letters* **100**, 59–76.

Geldmacher, J. & Hoernle, K. (2000). The 72 Ma geochemical evolution of the Madeira hotspot (eastern North Atlantic): recycling of Paleozoic (<500 Ma) oceanic lithosphere. *Earth and Planetary Science Letters* **183**, 73–92.

Geldmacher, J., Hoernle, K., van den Bogaard, P., Znkl, G & Garbe-Schönberg, D. (2001). Earlier history of the >70 Ma old Canary hotspot based on the temporal and geochemical evolution of the Selvagen Archipelago and neighbouring seamounts in the eastern North Atlantic. *Journal of Volcanology and Geothermal Research* **111**, 55–87.

Haase, K. M. (1996). The relationship between the age of the lithosphere and the composition of oceanic magmas: constraints on partial melting, mantle sources and the thermal structure of the plates. *Earth and Planetary Science Letters* **144**, 75–92.

Haase, K. M., Devey, C. W. & Goldstein, S. L. (1996). Two-way exchange between the Easter mantle plume and the Easter Microplate spreading axis. *Nature* **382**, 344–346.

Hanan, B. B., Kingsley, R. H. & Schilling, J.-G. (1986). Pb isotope evidence in the South Atlantic for migrating ridge–hotspot interactions. *Nature* **322**, 137–144.

Hauri, E. H., Lassiter, J. C. & DePaolo, D. J. (1996). Osmium isotope systematics of drilled lavas from Mauna Loa, Hawaii. *Journal of Geophysical Research* **101**, 11793–11806.

Hékinian, R., Stoffers, P., Ackermand, D., Révillon, S., Maia, M. & Bohn, M. (1999). Ridge–hotspot interaction: the Pacific–Antarctic Ridge and the Foundation Seamounts. *Marine Geology* **160**, 199–223.

Hémond, C., Arndt, N. T., Lichtenstein, U. & Hofmann, A. W. (1993). The heterogeneous Iceland plume: Nd–Sr–O isotopes and trace element constraints. *Journal of Geophysical Research* **98**, 15833–15850.

Hémond, C., Devey, C. W. & Chauvel, C. (1994*a*). Source compositions and melting processes in the Society and Austral plumes (South Pacific Ocean): element and isotope (Sr, Nd, Pb, Th) geochemistry. *Chemical Geology* **115**, 7–45.

Hémond, C., Hofmann, A. W., Heusser, G., Condomines, M., Raczek, I. & Rhodes, J. M. (1994*b*). U–Th–Ra systematics in Kilauea and Mauna Loa basalts, Hawaii. *Chemical Geology* **116**, 163–180.

Hoernle, K., Werner, R., Phipps Morgan, J., Garbe-Schonberg, D., Bryce, J. & Mrazek, J. (2000). Existence of complex spatial zonation in the Galapagos plume for at least 14 m.y. *Geology* **28**, 435–438.

Hofmann, A. W. (1988). Chemical differentiation of the Earth: the relationship between mantle, continental crust, and oceanic crust. *Earth and Planetary Science Letters* **90**, 297–314.

Hofmann, A. W. (1997). Mantle geochemistry: the message from oceanic volcanism. *Nature* **385**, 219–229.

Hofmann, A. W. & Jochum, K. P. (1996). Source characteristics derived from very incompatible trace elements in Mauna Loa and Mauna Kea basalts, Hawaii Scientific Drilling Project. *Journal of Geophysical Research* **101**, 11831–11839.

Hofmann, A. W. & White, W. M. (1982). Mantle plumes from ancient oceanic crust. *Earth and Planetary Science Letters* **57**, 421–436.

Hofmann, A. W., Jochum, K. P., Seufert, M. & White, W. M. (1986). Nb and Pb in oceanic basalts: new constraints on mantle evolution. *Earth and Planetary Science Letters* **79**, 33–45.

Janney, P. E. & Castillo, P. R. (1997). Geochemistry of Mesozoic Pacific mid-ocean ridge basalt: constraints on melt generation and the evolution of the Pacific upper mantle. *Journal of Geophysical Research* **102**, 5207–5229.

Janney, P. E. & Castillo, P. R. (1999). Isotope geochemistry of the Darwin Rise Seamounts and the nature of long-term mantle dynamics beneath the south central Pacific. *Journal of Geophysical Research* **104**, 10571–10589.

Janney, P. E., Macdougall, J. D., Natland, J. H. & Lynch, M. A. (2000). Geochemical evidence from the Pukapuka volcanic ridge system for a shallow enriched mantle domain beneath the South Pacific Superswell. *Earth and Planetary Science Letters* **181**, 47–60.

Jaques, A. L. & Green, D. H. (1980). Anhydrous melting of peridotite at 0–15 kb pressure and the genesis of tholeiitic basalts. *Contributions to Mineralogy and Petrology* **73**, 287–310.

Keller, R. A., Duncan, R. A. & Fisk, M. R. (1995). Geochemistry and $^{40}Ar/^{39}Ar$ geochronology of basalts from ODP Leg 145 (North Pacific Transect). In: Rea, D. K., Basov, I. A., Scholl, D. W. & Allan, J. A. (eds) *Proceedings of the Ocean Drilling Program, Scientific Results, 145*. College Station, TX: Ocean Drilling Program, pp. 333–343.

Keller, R. A., Fisk, M. R. & White, W. M. (2000). Isotopic evidence for Late Cretaceous plume–ridge interaction at the Hawaiian Hotspot. *Nature* **405**, 673–676.

Kempton, P. D. & Barry, T. L. (2001). Did the Hawaiian Plume interact with a mid-ocean ridge in the late Cretaceous? *Journal of Conference Abstracts* **6**, 466.

Kempton, P. D., Fitton, J. G., Saunders, A. D., Nowell, G. M., Taylor, R. N., Hardarson, B. S. & Pearson, G. (2000). The Iceland plume in space and time: a Sr–Nd–Pb–Hf study of the North Atlantic rifted margin. *Earth and Planetary Science Letters* **177**, 255–271.

Kingsley, R. H. & Schilling, J.-G. (1998). Plume–ridge interaction in the Easter–Salas y Gomez seamount chain–Easter Microplate system: Pb isotope evidence. *Journal of Geophysical Research* **103**, 24159–24177.

Kirkpatrick, R. J., Clague, D. A. & Freisen, W. (1980). Petrology and geochemistry of volcanic rocks, DSDP Leg 55, Emperor Seamount Chain. In: Jackson, E. D., Kosumi, I. *et al.* (eds) *Initial Reports of the Deep Sea Drilling Project, 55*. Washington, DC: US Government Printing Office, pp. 509–557.

Lanphere, M. A., Dalrymple, G. B. & Clague, D.A. (1980). Rb–Sr systematics of basalts from the Hawaiian–Emperor Volcanic Chain. In: Jackson, E. D., Kosumi, I. *et al.* (eds) *Initial Reports of the Deep Sea Drilling Project, 55*. Washington, DC: US Government Printing Office, pp. 695–706.

Lonsdale, P. (1988*a*). Paleogene history of the Kula Plate: offshore evidence and onshore implications. *Geological Society of America Bulletin* **100**, 733–754.

Lonsdale, P. (1988*b*). Geography and history of the Louisville Hotspot Chain in the southwest Pacific. *Journal of Geophysical Research* **93**, 3078–3104.

Lonsdale, P., Dieu, J. & Natland, J. (1993). Posterosional volcanism in the Cretaceous part of the Hawaiian hotspot trail. *Journal of Geophysical Research* **98**, 4081–4098.

Lugmair, G. & Galer, S. J. G. (1992). Age and isotopic relationships among the angrites Lewis Cliff 86010 and Angra dos Reis. *Geochimica et Cosmochimica Acta* **56**, 1673–1694.

Lyons, S. N., Sandwell, D. T. & Smith, W. H. F. (2000). Three-dimensional estimation of elastic thickness under the Louisville Ridge. *Journal of Geophysical Research* **105**, 13239–13252.

Macdougall, J. D. & Lugmair, G. W. (1986). Sr and Nd isotopes in basalts from the East Pacific Rise: significance for mantle heterogeneity. *Earth and Planetary Science Letters* **77**, 273–284.

Mahoney, J. J. (1987). An isotopic survey of Pacific oceanic plateaus: implications for their nature and origin. In: Keating, B. H., Fryer, P., Batiza, R. & Boehlert, G. W. (eds) *Seamounts, Islands and Atolls. Geophysical Monograph, American Geophysical Union* **43**, 207–220.

Mahoney, J. J., Frei, R., Tejada, M. L. G., Mo, X. X., Leat, P. T. & Nägler, T. F. (1998). Tracing the Indian Ocean mantle domain through time: isotopic results from old West Indian, East Tethyan, and South Pacific seafloor. *Journal of Petrology* **39**, 1285–1306.

Mammerickx, J. & Sharman, G. F. (1988). Tectonic evolution of the North Pacific during the Cretaceous Quiet Period. *Journal of Geophysical Research* **93**, 3009–3024.

McDonough, W. F. & Sun, S.-s. (1995). The composition of the Earth. *Chemical Geology* **120**, 223–253.

Morgan, W. J. (1971). Convection plumes in the lower mantle. *Nature* **230**, 42–43.

Nakamura, Y. & Tatsumoto, M. (1988). Pb, Nd and Sr isotopic evidence for a multicomponent source for rocks of Cook–Austral Islands and heterogeneities of mantle plumes. *Geochimica et Cosmochimica Acta* **52**, 2909–2924.

Niu, Y. & Batiza, R. (1997). Trace element evidence from seamounts for recycled oceanic crust in the Eastern Pacific mantle. *Earth and Planetary Science Letters* **148**, 471–483.

Niu, Y., Collerson, K. D., Batiza, R., Wendt, J. I. & Regelous, M. (1999). Origin of enriched-type mid-ocean ridge basalt at ridges far from mantle plumes: the East Pacific Rise at 11°20′N. *Journal of Geophysical Research* **104**, 7076–7087.

Niu, Y., Bideau, D., Hékinian, R. & Batiza, R. (2001). Mantle compositional control on the extent of mantle melting, crust production, gravity anomaly and ridge morphology: a case study at the Mid-Atlantic Ridge 33–35°N. *Earth and Planetary Science Letters* **186**, 383–399.

Parsons, B. & Sclater, J. G. (1977). An analysis of the variation of ocean floor bathymetry and heat flow with age. *Journal of Geophysical Research* **82**, 803–827.

Phipps Morgan, J. (1999). Isotope topology of individual hotspot basalt arrays: mixing curves or melt extraction trajectories? *Geochemistry, Geophysics, Geosystems* **1**, 1999GC000004.

Phipps Morgan, J. & Morgan, W. J. (1999). Two-stage melting and the geochemical evolution of the mantle: a recipe for mantle plum-pudding. *Earth and Planetary Science Letters* **170**, 215–239.

Pietruszka, A. J. & Garcia, M. O. (1999). A rapid fluctuation in the mantle source and melting history of Kilauea volcano inferred from the geochemistry of its historical summit lavas (1790–1982). *Journal of Petrology* **40**, 1321–1342.

Rea, D. K. & Dixon, J. M. (1983). Late Cretaceous and Paleogene tectonic evolution of the North Pacific Ocean. *Earth and Planetary Science Letters* **65**, 145–166.

Regelous, M. & Hofmann, A. W. (1999). Geochemistry of lavas from the Emperor Seamounts, and the geochemical evolution of Hawaiian magmatism since 85 Ma. *EOS Transactions, American Geophysical Union* **80**, F1102.

Regelous, M., Niu, Y., Wendt, J. I., Greig, A. & Collerson, K. D. (1999). Variations in the geochemistry of magmatism on the East Pacific Rise at 10°30′N since 800 ka. *Earth and Planetary Science Letters* **168**, 45–63.

Roden, M. F., Trull, T., Hart, S. R. & Frey, F. A. (1994). New He, Nd, Pb and Sr isotopic constraints on the constitution of the Hawaiian plume: results from Koolau Volcano, Oahu, Hawaii, USA. *Geochimica et Cosmochimica Acta* **58**, 1431–1440.

Royer, J.-Y. & Sandwell, D. T. (1989). Evolution of the Eastern Indian Ocean since the Late Cretaceous: constraints from satellite altimetry. *Journal of Geophysical Research* **94**, 13755–13782.

Salters, V. J. M. (1996). The generation of mid-ocean ridge basalts from the Hf and Nd isotope perspective. *Earth and Planetary Science Letters* **141**, 109–123.

Sandwell, D. T. & Smith, W. H. F. (1997). Marine gravity anomaly from Geosat and ERS 1 satellite altimetry. *Journal of Geophysical Research* **102**, 10039–10054.

Sandwell, D. T., Winterer, E. L., Mammerickx, J., Duncan, R. A., Lynch, D. A., Levitt, D. A. & Johnson, C. L. (1995). Evidence for diffuse extension of the Pacific Plate from Pukapuka Ridges and cross-grain gravity lineation. *Journal of Geophysical Research* **100**, 15087–15099.

Schilling, J.-G. (1991). Fluxes and excess temperatures of mantle plumes inferred from their interaction with migrating mid-ocean ridges. *Nature* **352**, 397–403.

Schilling, J.-G., Thompson, G., Kingsley, R. H. & Humphris, S. E. (1985). Hotspot–migrating ridge interactions along the South Atlantic: geochemical evidence. *Nature* **313**, 187–191.

Sims, K. W. W., DePaolo, D. J., Murrell, M. T., Baldridge, W. S., Goldstein, S. J. & Clague, D. (1995). Mechanisms of magma generation beneath Hawaii and mid-ocean ridges: uranium/thorium and samarium/neodymium isotopic evidence. *Science* **267**, 508–512.

Skovgaard, A. C., Storey, M., Baker, J., Blusztajn, J. & Hart, S. R. (2001). Osmium–oxygen isotopic evidence for a recycled and strongly depleted component in the Iceland mantle plume. *Earth and Planetary Science Letters* **194**, 259–275.

Sleep, N. H. (1984). Tapping of magmas from ubiquitous mantle heterogeneities: an alternative to mantle plumes? *Journal of Geophysical Research* **89**, 10029–10041.

Staudigel, H., Zindler, A., Hart, S. R., Leslie, T., Chen, C.-Y. & Clague, D. (1984). The isotope systematics of a juvenile intraplate volcano: Pb, Nd and Sr isotope ratios of basalts from Loihi Seamount, Hawaii. *Earth and Planetary Science Letters* **69**, 13–29.

Staudigel, H., Davies, G. R., Hart, S. R. & Marchant, K. M. (1995). Large-scale Sr, Nd and O isotopic anatomy of altered oceanic crust—DSDP/ODP Sites 417/418. *Earth and Planetary Science Letters* **130**, 169–185.

Stewart, R. J., Natland, J. H. & Glassley, W. R. (1973). Petrology of volcanic rocks recovered on DSDP Leg 19 from the North Pacific Ocean and the Bering Sea. In: Creager, J. S., Scholl, D. W. *et al.* (eds) *Initial Reports of the Deep Sea Drilling Project, 19*. Washington, DC: US Government Printing Office, pp. 615–627.

Stille, P., Unruh, D. M. & Tatsumoto, M. (1986). Pb, Sr, Nd and Hf isotopic constraints on the origin of Hawaiian basalts and evidence for a unique mantle source. *Geochimica et Cosmochimica Acta* **50**, 2303–2319.

Sun, S. & Hanson, G. N. (1975). Origin of Ross Island basanitoids and limitations upon the heterogeneity of mantle sources or alkali basalts and nephelinites. *Contributions to Mineralogy and Petrology* **52**, 77–106.

Sun, S.-s. & McDonough, W. F. (1989). Chemical and isotopic systematics of oceanic basalts: implications for mantle composition and process. In: Saunders, A. D. & Norry, M. J. (eds) *Magmatism in the Ocean Basins. Geological Society, London, Special Publications* **42**, 313–345.

Tatsumoto, M. (1978). Isotopic composition of lead in oceanic basalt and its implication to mantle evolution. *Earth and Planetary Science Letters* **38**, 63–87.

Thirlwall, M. F. (1995). Generation of the Pb isotopic characteristics of the Iceland plume. *Journal of the Geological Society, London* **152**, 991–996.

Watson, S. & McKenzie, D. (1991). Melt generation by plumes: a study of Hawaiian volcanism. *Journal of Petrology* **32**, 501–537.

Watts, A. B., Weissel, J. K., Duncan, R. A. & Larson, R. L. (1988). Origin of the Louisville Ridge and its relationship to the Eltanin Fracture Zone System. *Journal of Geophysical Research* **93**, 3051–3077.

Wendt, J. I., Regelous, M., Niu, Y., Hékinian, R. & Collerson, K. D. (1999). Geochemistry of lavas from the Garrett Transform Fault: insights into mantle heterogeneity beneath the eastern Pacific. *Earth and Planetary Science Letters* **173**, 271–284.

White, W. M. (1993). $^{238}U/^{204}Pb$ in MORB and open system evolution of the depleted upper mantle. *Earth and Planetary Science Letters* **115**, 211–226.

White, W. M. & Duncan, R. A. (1996). Geochemistry and geochronology of the Society Islands: new evidence for deep mantle recycling. In: Basu, A. & Hart, S. R. (eds) *Earth Processes: Reading the Isotopic Code. Geophysical Monograph, American Geophysical Union* **95**, 183–206.

White, W. M. & Hofmann, A. W. (1982). Sr and Nd isotope geochemistry of oceanic basalts and mantle evolution. *Nature* **296**, 821–825.

White, W. M., McBirney, A. R. & Duncan, R. A. (1993). Petrology and geochemistry of the Galapagos Islands: portrait of a pathological mantle plume. *Journal of Geophysical Research* **98**, 19533–19563.

Worsley, J. R. (1973). Calcareous nannofossils: Leg 19 of the Deep Sea Drilling Project. In: Creager, J. S., Scholl, D. W. *et al.* (eds) *Initial Reports of the Deep Sea Drilling Project, 19*. Washington, DC: US Government Printing Office, pp. 741–750.